With a similar goal in mind, we previously constructed M13 bacteriophage libraries (Library I and Library II) displaying mutant TNFs randomized at amino acid positions 29, 31, 32, 145, 146 and 147 or at positions 84–89 of TNF, and succeeded in isolating agonistic- and antagonistic-mutant TNFs from these libraries [11,12]. Particularly, the TNFR1-selective antagonist mutTNF-T2 showed almost same therapeutic effect as the anti-TNF biologics in a hepatitis model [13].

Currently, generation of a phage-displayed library with large repertoire (>10^8) is impeded by the limited transformation efficiency of *Escherichia coli* (*E. coli*). As a result, it is difficult to construct a high quality mutant library ($20^6 = 6.4 \times 10^7$) that is randomized at more than seven different amino acid residues and includes almost all clones. To overcome this problem, here we have developed a novel protein engineering strategy (gene shuffling method) for creation of functional mutant proteins. To achieve our goal, we first constructed two types of phage libraries displaying mutant TNFs, in each of which six amino acids residues in the predicted receptor binding sites were replaced with other amino acid residues, and these phage display libraries were subsequently subjected to several rounds of panning against TNFR1 and TNFR2, respectively, using a surface plasmon resonance analyzer (BIAcore). After several rounds of panning, we obtained two libraries, each one containing enriched number of a TNF receptor-specific high affinity clones. Next, we utilized these enriched libraries to construct high quality TNF receptor-specific shuffling libraries using a gene shuffling method. Finally, panning of these shuffling libraries against TNFR1 and TNFR2, respectively, have allowed us to isolate TNF mutants with greater receptor-selectivity and enhanced receptor-specific bioactivity than the previously isolated TNFR1-selective mutant R1-5 and TNFR2-selective mutant R2-3 [12].

Materials and methods

Cell culture. HEp-2 cells (a human fibroblast cell line) were provided by the Cell Resource Center for Biomedical Research (Tohoku University, Sendai, Japan) and were maintained in RPMI 1640 medium (Sigma-Aldrich Japan, Tokyo, Japan) supplemented with 10% FBS and antibiotics cocktail (penicillin 10,000 units/ml, streptomycin 10 mg/ml, and amphotericin B 25 μg/ml; Nacalai tesque, Kyoto, Japan). hTNFR2/mFas-preadipocyte (mouse preadipocyte cell expressing a chimeric receptor, which consist of the extracellular and transmembrane domain of human TNFR2 and the intracellular domain of mouse Fas) cells were established previously in our laboratory [14] and were maintained in D-MEM (Wako Pure Chemical Industries, Osaka, Japan) supplemented with blasticidin S HCl (5 μg/ml Sigma-Aldrich Japan, Tokyo, Japan), 10% FBS, 1 mM sodium pyruvate, 5×10^{-5} M 2-mercaptoethanol, and antibiotic cocktail.

Selection of TNF receptor-selective mutants from the mutant TNF phage display library by panning. Human TNFR1 Fc chimera or human TNFR2 Fc chimera (R&D systems, Minneapolis, MN) was immobilized onto a CM3 sensor chip (GE Healthcare, Buckinghamshire, UK) as described previously [11,12]. The phage display library (1×10^{11} CFU/100 μl) was injected over the sensor chip at a flow rate of 3 μl/min on BIAcore. After binding, the chip was rinsed until the association phase was reached. Elution was carried out using 4 μl of 10 mM glycine–HCl. The eluted phage pool was neutralized with 1 M Tris–HCl (pH 6.9). Next, the phages in the eluted pool were amplified in the *E. coli* TG1. The panning, elution and amplification steps were repeated twice. Subsequently, single clones were isolated from the phage pool, and the DNA sequences of phagemids purified from the single clones were analyzed.

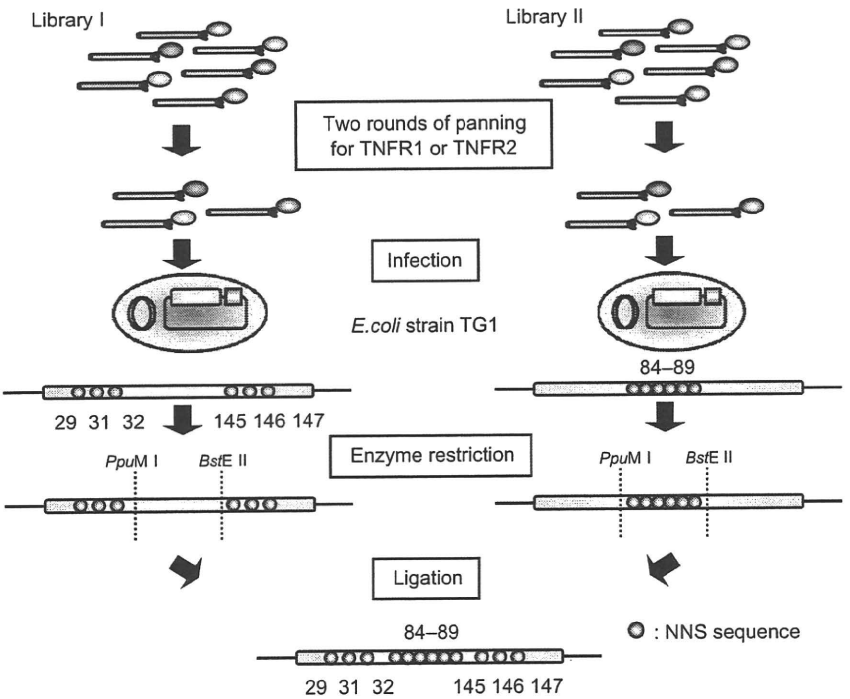

Fig. 1. Construction of the Gene Shuffling Library. Schematic description of the methods used to construct the Gene Shuffling Libraries A and B from two parent mutant TNF libraries, each one of which was created by replacing the codon of the amino acid residue at positions 29, 31, 32, 145, 146 and 147 (Library I) or at positions 84, 85, 86, 87, 88 and 89 (Library II) of TNF with the randomized codon NNS (where N and S represent G/A/T/C or G/C, respectively) to obtain all twenty amino acid substitutions at each position. NNS encodes all 20 different amino acids. Mutations were introduced by PCR using the lysine-deficient mutant TNF as the template as described in Materials and methods.

Construction of mutant TNF phage library (Gene Shuffling Library). The pCANTAB phagemid vector encoding a lysine-deficient mutant TNF which was created previously was used as a template for library construction [15]. First, two types of phage libraries, displaying mutant TNFs containing random substitutions of amino acid residues at positions 29, 31, 32, 145, 146 and 147 (Library I), and at positions 84, 85, 86, 87, 88 and 89 (Library II), were prepared using polymerase chain reaction (PCR) as described earlier [11,12]. Each library was then subjected to two rounds of panning against TNFR1 to concentrate TNFR1-specific high-affinity mutant TNFs. Next, we purified all plasmids from each concentrated libraries. These two pools of purified plasmids were digested with the restrict enzymes (*Ppu*MI, *Bst*EII), DNA inserts were purified and then ligated to a pY03′ phagemid vector to construct a randomized library (Shuffling Library A) that contained mutations at twelve different amino acid residues (see Fig. 1). We also prepared a second randomized library (Shuffling Library B) by following the same protocol and using TNFR2 for panning.

Competitive ELISA. Inhibition of wtTNF binding to the TNFR1 and TNFR2 by a TNFR1 or TNFR2-selective mutant was measured using ELISA as described previously [16]. The wtTNF-FLAG, a FLAG tag fusion protein of human TNF [16], was used as a marker protein. Briefly, the immune assay plates (NUNC, Roskilde, Denmark) were coated with 5 μg/ml goat anti-human IgG antibody (MP Biomedicals, Aurora, OH) and incubated with 0.2 μg/ml of either the human TNFR1 or the human TNFR2. After blocking the non-specific binding sites, a pre-made mixture containing 100 ng/ml of wtTNF-FLAG and various concentrations of a given TNF mutant was added to the wells. After 2 h of incubation at room temperature, the wells were washed. Next, 0.5 μg/ml biotinylated anti-FLAG M2 antibody was added to each well and then the plate was incubated for an additional period of 2 h at room temperature. Wells were washed and then incubated with the horseradish peroxidase-coupled streptavidin (Zymed Lab. Inc., South San Francisco, CA) for 30 min at room temperature. The remaining bound wtTNF-FLAG was quantified as described above.

Assay for cytotoxicity mediated via TNFR1 and TNFR2. To measure cytotoxicity mediated via the TNFR1, HEp-2 cells (4×10^4 cells/well) were cultured in 96-well plates (NUNC, Roskilde, Denmark) in presence of a given TNF mutant, serially diluted human wtTNF (Peprotech, Rocky Hill, NJ), and with 100 μg/ml cycloheximide for 18 h, and cytotoxicity was assessed by using the methylene blue assay as described previously [17]. To measure cytotoxicity mediated via the TNFR2, hTNFR2/mFas-preadipocyte cells (1×10^4 cells/well) were cultured in the 96-well plates (NUNC) in presence of a given TNF mutant and serially diluted human wtTNF for 48 h, and then cell survival was determined by using the methylene blue assay.

Results and discussion

In this study, to overcome the barrier of limited transformation efficiency of *E. coli* in the preparation of high quality phage display libraries, we adopted a novel protein engineering technology in which amino acid residues at 12 different places were randomly substituted using a gene shuffling method to enhance the usefulness of the phage display technique.

Fig. 1 schematically summarizes the protocol used for constructing a novel TNF gene shuffling library. First, we prepared two phage libraries displaying mutant TNFs, in each of which six different amino acid residues (residues at positions 29, 3, 32, 145, 146 and 147 for Library I; residues at positions from 84 to 89 for Library II) present in the receptor binding site of TNF, previously identified by point mutation analysis and X-ray crystallography, were randomly substituted with other amino acid residues [11,12]. The phage libraries expressing mutant TNFs were constructed by two-step PCR as described in the Materials and methods. We confirmed that the phage Libraries I and II consisted of 8×10^6 and 6×10^6 independent clones, respectively (*data not shown*). Next, to enrich for TNFR1 binding mutants, we subjected each library to two rounds of panning using TNFR1 and recovered phage clones with high affinity to TNFR1. We used a gene shuffling method to construct the mutant TNF Shuffling Library A from these libraries, which consist of high affinity clones to TNFR1 (see Fig. 1). In the similar manner, we constructed the Shuffling Library B by carrying out panning using TNFR2. Amino acid analysis of eight randomly picked clones from each library revealed that each one of them was a mutant containing amino acid substitutions at 12 residues (*results not shown*). To concentrate TNFR1-selective mutant TNFs, the Shuffling Library A was subjected to two rounds of panning against TNFR1 using the BIAcore biosensor. After the second panning, supernatants of *E. coli* TG1 included phagemid were randomly collected and performed the screening by ELISA and bioassay to analyze their bioactivity and affinity against TNFR1 (*data not shown*). As a result, we identified six TNFR1-selective, high affinity clones, R1-15 to R1-20 (Table 1). Similarly, we identified three TNFR2-selective candidates (R2-14 to R2-16) from the Shuffling Library B (Table 1). The fact that the amino acid residue at position 87 in all active TNF receptor-selective candidates was a Tyr residue (Table 1), it suggests that Tyr87 is an important residues

Table 1
Substituted residues and affinities of TNF receptor-selective mutant candidates.

	Amino acid sequence												Relative affinity (%)[a]		
	29	31	32	84	85	86	87	88	89	145	146	147	TNFR1	TNFR2	TNFR1/TNFR2
wtTNF	L	R	R	A	V	S	Y	Q	T	A	E	S	100.0	100.0	1.0
R1-5[b]	K	A	G	–	–	–	–	–	–	–	S	T	82.0	2.0×10^{-2}	4.1×10^3
R1-15	R	N	Y	S	–	R	–	N	P	–	–	–	115.7	6.0×10^{-2}	1.9×10^3
R1-16	T	Q	Y	T	P	G	–	S	H	–	A	H	8.6	6.0×10^{-2}	1.4×10^2
R1-17	R	T	F	S	P	L	–	R	Q	S	S	T	54.2	6.0×10^{-2}	9.0×10^2
R1-18	K	N	F	S	S	H	–	T	H	–	–	–	53.9	1.0×10^{-1}	5.4×10^2
R1-19	S	N	Y	–	–	–	–	–	–	–	V	–	138.7	8.0×10^{-1}	1.7×10^3
R1-20	T	–	Y	S	H	T	–	P	S	S	Q	A	170.5	3.0×10^{-2}	5.7×10^3
R2-3[c]	–	–	–	–	–	–	–	–	–	R	–	T	<0.1	33.4	<0.0029
R2-14	–	–	–	–	P	–	–	N	S	S	A	D	1.6	103.7	0.0154
R2-15	–	–	–	S	Q	A	–	N	–	I	G	D	<0.1	141.8	<0.0007
R2-16	–	–	–	–	–	–	–	–	–	H	S	D	1.4	91.7	0.0152

Comparison of the amino acid residues of the wild-type and mutant TNFs; conserved residues are indicated using a dash.
[a] Concentration of mutant TNF required for 50% inhibition of maximal binding of wtTNF-FLAG.
[b] A TNFR1-selective mutant, which was isolated previously from the existing phage library (Library I).
[c] A TNFR2-selective mutant, which was isolated obtained from the existing phage library (Library I).

for receptor binding, which is in good agreement with the previous report [8–10].

To determine the properties of the receptor-selective candidates, we purified all the candidate TNF mutants as recombinant proteins using a general recombinant protein technology [11,12,15,18]. After each recombinant mutant TNF was expressed in *E. coli* BL21λDE3 and purified to homogeneity, we used gel electrophoresis and gel filtration chromatography to confirm that each of them, like the wtTNF, displayed MW of 17 kDa and formed a homotrimeric complex (*results not shown*). We next used a competitive ELISA to examine the binding properties of the mutant TNFs to the TNF receptors, and the results are summarized in Table 1. As summarized, all TNFR1-selective candidates showed lower affinity for TNFR2 than the wtTNF. On the other hand, affinities of the clones R1-15, R1-19, and R1-20 for TNFR1 were better than that the wtTNF. Especially, affinity of the clone R1-20 for TNFR1 was more than 1.7-fold higher than that of the wtTNF and was about 2-fold higher than that of the TNF mutant R1-5, which was previously identified from the Library I [12]. Additionally, selectivity of R1-20 for TNFR1 was higher than that of the R1-5. Next, we evaluated affinity of the TNFR2-selective mutants for TNFR2 (Table 1). Our results revealed that the clones R2-14, R2-15 and R2-16 bound to TNFR2 more strongly than the TNF mutant R2-3, which was previously isolated in our laboratory [12]. Especially, the TNF mutant R2-15 bound to TNFR2 with an affinity that was 1.4-fold higher than that of the wtTNF. R2-15 also showed superior TNFR2-selectivity than R2-3. Thus, by using the gene shuffling libraries, we were able to isolate TNF mutants that were highly receptor-selective. The receptor-selective TNF mutants R1-20 and R2-15 contained amino acid substitutions at 10 and 7 places, respectively. A point mutation analysis study of TNF suggested that the amino acid residues near position 140 are essential for TNFR1 binding [8,10,12]. In agreement with this report, we found that the residue at position 145 in the TNFR1-specific mutants is mostly retained or contained conservative amino acid substitutions, whereas more than one residues at positions 145, 146 and 147 in the TNFR2-selective mutants contained non-conservative amino acid substitutions. On the other hand, the amino acids residues near positions 30 and 80 were mostly conserved in the TNFR2-specific mutants, but not in the TNFR1-specifc mutants, suggesting that these amino acid residues might play important roles in TNFR2 binding [12]. Thus, this is the first report describing the creation of highly receptor-selective TNF mutants, namely R1-20 and R2-15, from a randomized mutant TNF library containing amino acid substitutions at 12 different amino acid residues. These results clearly demonstrate the usefulness of the developed method, which combines both phage display and gene shuffling techniques.

Next, we examined the receptor-selective bioactivities of the TNF mutants R1-20 and R2-15, each one of which showed highest receptor-selectivity, and the results are shown in Fig. 2 and Table 2. TNFR1-mediated cytotoxicity induced by the TNF mutant R1-20, as measured *in vitro* using the Hep-2 cells, was 7-fold and 2.2-fold higher than those of the mutant R1-5 and wtTNF, respectively (Fig. 2A and Table 2). Next, we evaluated the TNFR2-mediated activity of R1-20 using the hTNFR2/mFas-preadipocyte cells, which were previously constructed in our laboratory [14]. As expected, R1-20 hardly exhibited bioactivity via TNFR2, and the activity was much lower than that of the wtTNF (Fig. 2B and Table 2). On the other hand, the bioactivity of the TNFR2-selective mutant R2-15 via TNFR1 was 1000-fold lower than that of the wtTNF (Fig. 2C). The bioactivity of R2-15 via TNFR2 was, however, 2.5-fold higher than that of the wtTNF and more than 15-fold higher than that of the R2-3 mutant (Fig. 2D and Table 2). Remarkably, the bioactivity of R2-15 was higher that that of the R2-3, both of which are TNFR2-specific TNF mutants (Fig. 2D and Table 2).

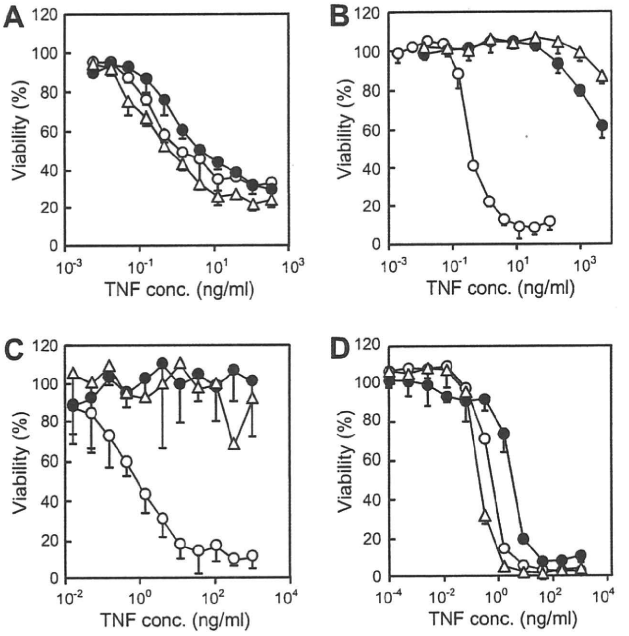

Fig. 2. Bioactivity of the receptor-selective mutants. The receptor-specific bioactivity (% viability) was measured following the treatment of HEp-2 or hTNFR2/mFas-preadipocyte cells with the wild-type or mutant TNF by using the methylene blue staining procedure as described in Materials and methods. (A) and (C) TNFR1-mediated bioactivity was measured using the HEp-2 cells. (B) and (D) TNFR2-mediated bioactivity was measured using the hTNFR2/mFas-preadipocyte cells. In (A) and (B) open circle, wtTNF; closed circle, R1-5; and open triangle, R1-20. In (C) and (D) open circle, wtTNF; closed circle, R2-3; and open triangle, R2-15.

Table 2
Bioactivity of receptor-selective mutants.

	TNFR1[a]		TNFR2[b]	
	EC50 (ng/ml)	Relative (%)	EC50 (ng/ml)	Relative (%)
wtTNF	1.3	100.0	0.4	100.0
R1-5	4.4	29.5	$>5.0 \times 10^5$	$<8.0 \times 10^{-5}$
R1-20	0.6	216.7	$>5.0 \times 10^5$	$<8.0 \times 10^{-5}$
R2-3	$>1.0 \times 10^3$	<0.1	3.1	13.0
R2-15	$>1.0 \times 10^3$	<0.1	0.2	200.0

The bioactivity values were determined from the results shown in Fig. 2 and are shown here as relative values (% wtTNF). Each value shown is mean ± SD ($n = 3$).

[a] TNFR1-mediated bioactivity was determined by a cytotoxicity assay as described in Materials and methods using the HEp-2 cells.

[b] TNFR2-mediated bioactivity was determined by a cytotoxicity assay as described in Materials and methods using the hTNFR2/mFas-preadipocyte cells.

Thus, by using the combined technology described in this study, we were able to identify TNF mutants with improved TNF receptor-selectivity and enhanced bioactivity than the existing TNF mutants.

Presently, both the underlying mechanism of signal transduction via each TNF receptor, and the relationship between the TNF receptors and onset of TNF-related diseases remain unclear. We anticipate that the TNF receptor-selective TNF mutants found in this study could be used as tools to analyze the receptor-specific signal transduction pathways. Additionally, we believe that the technology described here would be easily applicable to many disease-related proteins of unknown function. Thus, by creating structurally diverse protein libraries, we could rapidly identify therapeutically valuable proteins, which might lead to the development of effective and safe drugs in the near future.

Acknowledgments

This study was supported in part by Grants-in-Aid for Scientific Research from the Ministry of Education, Culture, Sports, Science and Technology of Japan, and by Grants-in-Aid for Scientific Research from Japan Society for the Promotion of Science (JSPS). In addition, this study was also supported in part by Health Labour Sciences Research Grants from the Ministry of Health, Labor and Welfare of Japan, Health Sciences Research Grants for Research on Publicly Essential Drugs and Medical Devices from the Japan Health Sciences Foundation, as well as The Nagai Foundation Tokyo.

References

[1] H. Wajant, K. Pfizenmaier, P. Scheurich, Tumor necrosis factor signaling, Cell Death Differ. 10 (2003) 45–65.
[2] Y. Muto, K.T. Nouri-Aria, A. Meager, G.J. Alexander, A.L. Eddleston, R. Williams, Enhanced tumour necrosis factor and interleukin-1 in fulminant hepatic failure, Lancet 2 (1988) 72–74.
[3] M. Feldmann, R.N. Maini, Lasker Clinical Medical Research Award. TNF defined as a therapeutic target for rheumatoid arthritis and other autoimmune diseases, Nat. Med. 9 (2003) 1245–1250.
[4] J. Keane, S. Gershon, R.P. Wise, E. Mirabile-Levens, J. Kasznica, W.D. Schwieterman, J.N. Siegel, M.M. Braun, Tuberculosis associated with infliximab, a tumor necrosis factor alpha-neutralizing agent, N. Engl. J. Med. 345 (2001) 1098–1104.
[5] N. Shakoor, M. Michalska, C.A. Harris, J.A. Block, Drug-induced systemic lupus erythematosus associated with etanercept therapy, Lancet 359 (2002) 579–580.
[6] T. Weiss, M. Grell, K. Siemienski, F. Muhlenbeck, H. Durkop, K. Pfizenmaier, P. Scheurich, H. Wajant, TNFR80-dependent enhancement of TNFR60-induced cell death is mediated by TNFR-associated factor 2 and is specific for TNFR60, J. Immunol. 161 (1998) 3136–3142.
[7] M. Fotin-Mleczek, F. Henkler, D. Samel, M. Reichwein, A. Hausser, I. Parmryd, P. Scheurich, J.A. Schmid, H. Wajant, Apoptotic crosstalk of TNF receptors: TNF-R2-induces depletion of TRAF2 and IAP proteins and accelerates TNF-R1-dependent activation of caspase-8, J. Cell Sci. 115 (2002) 2757–2770.
[8] X. Van Ostade, J. Tavernier, W. Fiers, Structure–activity studies of human tumour necrosis factors, Protein Eng. 7 (1994) 5–22.
[9] X.M. Zhang, I. Weber, M.J. Chen, Site-directed mutational analysis of human tumor necrosis factor-alpha receptor binding site and structure–functional relationship, J. Biol. Chem. 267 (1992) 24069–24075.
[10] J. Yamagishi, H. Kawashima, N. Matsuo, M. Ohue, M. Yamayoshi, T. Fukui, H. Kotani, R. Furuta, K. Nakano, M. Yamada, Mutational analysis of structure–activity relationships in human tumor necrosis factor-alpha, Protein Eng. 3 (1990) 713–719.
[11] H. Shibata, Y. Yoshioka, A. Ohkawa, K. Minowa, Y. Mukai, Y. Abe, M. Taniai, T. Nomura, H. Kayamuro, H. Nabeshi, T. Sugita, S. Imai, K. Nagano, T. Yoshikawa, T. Fujita, S. Nakagawa, A. Yamamoto, T. Ohta, T. Hayakawa, T. Mayumi, P. Vandenabeele, B.B. Aggarwal, T. Nakamura, Y. Yamagata, S. Tsunoda, H. Kamada, Y. Tsutsumi, Creation and X-ray structure analysis of the tumor necrosis factor receptor-1-selective mutant of a tumor necrosis factor-alpha antagonist, J. Biol. Chem. 283 (2008) 998–1007.
[12] Y. Mukai, H. Shibata, T. Nakamura, Y. Yoshioka, Y. Abe, T. Nomura, M. Taniai, T. Ohta, S. Ikemizu, S. Nakagawa, S. Tsunoda, H. Kamada, Y. Yamagata, Y. Tsutsumi, Structure–function relationship of tumor necrosis factor (TNF) and its receptor interaction based on 3D structural analysis of a fully active TNFR1-selective TNF mutant, J. Mol. Biol. 385 (2009) 1221–1229.
[13] H. Shibata, Y. Yoshioka, A. Ohkawa, Y. Abe, T. Nomura, Y. Mukai, S. Nakagawa, M. Taniai, T. Ohta, T. Mayumi, H. Kamada, S. Tsunoda, Y. Tsutsumi, The therapeutic effect of TNFR1-selective antagonistic mutant TNF-α in murine hepatitis models, Cytokine 44 (2008) 229–233.
[14] Y. Abe, T. Yoshikawa, H. Kamada, H. Shibata, T. Nomura, K. Minowa, H. Kayamuro, K. Katayama, H. Miyoshi, Y. Mukai, Y. Yoshioka, S. Nakagawa, S. Tsunoda, Y. Tsutsumi, Simple and highly sensitive assay system for TNFR2-mediated soluble- and transmembrane-TNF activity, J. Immunol. Methods 335 (2008) 71–78.
[15] Y. Yamamoto, Y. Tsutsumi, Y. Yoshioka, T. Nishibata, K. Kobayashi, T. Okamoto, Y. Mukai, T. Shimizu, S. Nakagawa, S. Nagata, T. Mayumi, Site-specific PEGylation of a lysine-deficient TNF-alpha with full bioactivity, Nat. Biotechnol. 21 (2003) 546–552.
[16] C.R. Brunetti, M. Paulose-Murphy, R. Singh, J. Qin, J.W. Barrett, A. Tardivel, P. Schneider, K. Essani, G. McFadden, A secreted high-affinity inhibitor of human TNF from Tanapox virus, Proc. Natl. Acad. Sci. USA 100 (2003) 4831–4836.
[17] Y. Tsutsumi, T. Kihira, S. Tsunoda, T. Kanamori, S. Nakagawa, T. Mayumi, Molecular design of hybrid tumour necrosis factor alpha with polyethylene glycol increases its anti-tumour potency, Br. J. Cancer 71 (1995) 963–968.
[18] H. Shibata, Y. Yoshioka, S. Ikemizu, K. Kobayashi, Y. Yamamoto, Y. Mukai, T. Okamoto, M. Taniai, M. Kawamura, Y. Abe, S. Nakagawa, T. Hayakawa, S. Nagata, Y. Yamagata, T. Mayumi, H. Kamada, Y. Tsutsumi, Functionalization of tumor necrosis factor-alpha using phage display technique and PEGylation improves its antitumor therapeutic window, Clin. Cancer Res. 10 (2004) 8293–8300.

Biomaterials 30 (2009) 6638–6647

Contents lists available at ScienceDirect

Biomaterials

journal homepage: www.elsevier.com/locate/biomaterials

The treatment of established murine collagen-induced arthritis with a TNFR1-selective antagonistic mutant TNF

Hiroko Shibata [a,b,1], Yasuo Yoshioka [c,1], Yasuhiro Abe [a,1], Akiko Ohkawa [a], Tetsuya Nomura [a,d], Kyoko Minowa [a], Yohei Mukai [a,d], Shinsaku Nakagawa [d], Madoka Taniai [e], Tsunetaka Ohta [e], Haruhiko Kamada [a,c], Shin-ichi Tsunoda [a,c,*], Yasuo Tsutsumi [a,c,d]

[a] Laboratory of Pharmaceutical Proteomics, National Institute of Biomedical Innovation (NIBIO), 7-6-8 Saito-Asagi, Ibaraki, Osaka 567-0085, Japan
[b] National Institute of Health Sciences (NIHS), Kamiyoga 1-18-1, Setagaya-ku, Tokyo 158-8501, Japan
[c] The Center for Advanced Medical Engineering and Informatics, Osaka University. 1-6 Yamadaoka, Suita, Osaka 565-0871, Japan
[d] Graduate School of Pharmaceutical Sciences, Osaka University, 1-6 Yamadaoka, Suita, Osaka 565-0871, Japan
[e] Hayashibara Biochemical Laboratories, Inc., 675-1 Fujisaki, Okayama 702-8006, Japan

ARTICLE INFO

Article history:
Received 7 July 2009
Accepted 28 August 2009
Available online 17 September 2009

Keywords:
Rheumatoid arthritis
Cytokines
Cytokine receptors
Tumor necrosis factor

ABSTRACT

Blocking the binding of TNF-α to TNF receptor subtype-1 (TNFR1) is an important strategy for the treatment of rheumatoid arthritis (RA). We recently succeeded in developing a TNFR1-selective antagonistic TNF mutant, R1antTNF. Here, we report the anti-inflammatory effects of R1antTNF in a murine collagen-induced arthritis model. To improve the *in vivo* stability of R1antTNF, we first engineered PEG (polyethylene glycol)-modified R1antTNF (PEG–R1antTNF). In prophylactic protocols, PEG–R1antTNF clearly improved the incidence, and the clinical score of arthritis due to its long plasma half-life. Although, the effect of PEG–R1antTNF on the incidence and production of IL1-β was less than that of the existing TNF-blocking drug Etanercept, its effect on severity was almost as marked as Etanercept. Interestingly, in therapeutic protocols, PEG–R1antTNF showed greater therapeutic effect than Etanercept. These data suggest that the anti-inflammatory effects of PEG–R1antTNF depend on the stage of arthritis. Recently, there has been much concern over the reactivation of viral infection caused by TNF blockade. Unlike Etanercept, PEG–R1antTNF did not reactivate viral infection. Together, these results indicate that selective inhibition of TNF/TNFR1 could be effective in treating RA and that PEG–R1antTNF could serve as a promising anti-inflammatory drug for this purpose.

1. Introduction

Rheumatoid arthritis (RA) is an autoimmune inflammatory disease affecting approximately 1% of the population world-wide, with over 60 million people suffering from this disorder [1]. Although the fundamental cause of RA remains unclear, among inflammatory cytokines, TNF-α is believed to be involved in the development and exacerbation of the pathology [2–4]. Currently, TNF-neutralization therapies using Etanercept (Enbrel®), a soluble Fc-TNF receptor (TNFR) 2 fusion protein, or Infliximab (Remicade®), a TNF-specific monoclonal antibody, have proven successful as a strategy for treatment of RA [5–7]. Because TNF blockade not only improves symptoms but also suppresses joint destruction [8], it is viewed as a highly effective therapeutic approach. However, therapeutic efficacy may be accompanied by side effects, such as congestive heart failure [9], demyelinating disease [10], and lupus-like syndrome [11]. Most notably, the use of TNF blockade is associated with an increased risk of bacterial and virus infection [12,13] and lymphoma development [14] because TNF-dependent host defense functions are also inhibited. Therefore, to overcome these problems, development of a new therapeutic strategy is highly desirable.

TNF exerts its biological functions by binding to one of two receptors, TNFR1 or TNFR2. Mori et al. reported that the incidence and severity of arthritis was lower and milder in TNFR1-knockout mice than in wild-type mice [15]. Additionally, previous studies demonstrated that transgenic mice with enforced expression of human TNF developed severe arthritis [16,17]. Thus, the involvement of TNFR1 in arthritis pathogenesis

* Corresponding author. Laboratory of Pharmaceutical Proteomics, National Institute of Biomedical Innovation (NIBIO), 7-6-8 Saito-Asagi, Ibaraki, Osaka 567-0085, Japan. Tel.: +81 72 641 9811; fax: +81 72 641 9817.
E-mail address: tsunoda@nibio.go.jp (S.-i. Tsunoda).
[1] These authors contributed equally to the work.

0142-9612/$ – see front matter © 2009 Elsevier Ltd. All rights reserved.
doi:10.1016/j.biomaterials.2009.08.041

is strongly implicated, because human TNF binds and activates only murine TNFR1 but not TNFR2. On the other hand, TNFR2 was shown to be crucial for the antigen-stimulated activation and proliferation of T cells [18–20], essential for cell-mediated immune responses to infection. Additionally, transmembrane TNF (tmTNF), the prime activating ligand of TNFR2 [21], was reported to be sufficient to control *Mycobacterium tuberculosis* infection [22,23], indicating the importance of TNF/TNFR2 function in this bacterial infection. Based on these studies, blocking TNF/TNFR1- but not TNF/TNFR2-interations is emerging as an effective and safe strategy for treating inflammatory diseases, which might overcome the risk of infections associated with the use of the currently available TNF blockades [24]. However, because TNFR1-selective antagonists had not yet been developed, the efficacy of this strategy has not been verified thus far.

With this in mind, we generated the TNFR1-selective antagonistic TNF-mutant, R1antTNF, based on human TNF [25]. This agent binds only to TNFR1, and inhibits multiple TNF functions mediated through that receptor *in vitro* and *in vivo* [26]. Therefore, we propose that R1antTNF may be a useful therapeutic agent in chronic inflammatory diseases. However, when administered intravenously, like wild-type TNF, R1antTNF has a very short half-life in the plasma of mice (about 10 min). To overcome this limitation, we recently developed a site-specific PEGylation process that significantly improves the *in vivo* stability and therapeutic effect of TNF without loss of bioactivity [27–29]. The application of this technology to R1antTNF aimed to lengthen the plasma half-life and improve the therapeutic effects of R1antTNF. In the present study, after confirming the inhibitory effect of R1antTNF on TNF-induced osteoclast differentiation in an RA-related *in vitro* assay, we prepared such PEGylated R1antTNF, and assessed its therapeutic effects in an established arthritis model.

2. Materials and methods

2.1. Mice

BALB/c, DBA/1J and C57/BL6 mice were purchased from SLC Japan and maintained under specific pathogen-free conditions. All experimental protocols for animal studies were in accordance with "*Principles of Laboratory Animal Care*" (National Institutes of Health publication no. 85-23, revised 1985: http://grants1.nih.gov/grants/olaw/references/phspol.htm) and our institutional guidelines.

2.2. Expression and purification of R1antTNF

A plasmid encoding the R1antTNF gene under the control of the T7 promoter was prepared and the molecule produced following procedures for the expression and purification of recombinant proteins described previously [28]. Briefly, R1antTNF was over-expressed in *E. coli* BL21(DE3), recovered from the inclusion body, washed with 2.5% Triton X-100 and 0.5 M NaCl in TES buffer, and then solubilized in 6 M guanidine–HCl, 0.1 M Tris–HCl, pH 8.0, and 2 mM EDTA. The solubilized protein was reduced with 10 mg/ml dithioerythritol for 4 h at RT, and then refolded by 100-fold dilution in a refolding buffer [100 mM Tris–HCl, 2 mM EDTA, 0.5 M arginine, and oxidized glutathione (551 mg/L)]. After dialyzing against 20 mM Tris–HCl, pH 7.4, containing 100 mM urea, the active trimeric proteins were purified by Q-Sepharose chromatography (GE Healthcare Bioscience, Tokyo, Japan). Additional gel filtration chromatography (Superose 12, GE Healthcare Bioscience) was performed to further purify each protein. The endotoxin level in the purified R1antTNF was determined to be <300 pg/mg.

2.3. In vitro osteoclastogenesis assay

Bone marrow cells prepared from DBA/1J mice were suspended in MEM (Sigma–Aldrich Japan, Tokyo, Japan) containing 10% FBS and cultured at 1.5×10^4 cells/cm^2 in the presence of M-CSF (50 ng/ml; PeproTech, Rocky Hill, NJ). The cells were cultured for 3 days, then harvested and seeded into 48-well plates (1.5×10^4 cells/well), and maintained for 5 days in the presence of diluted R1antTNF, or mouse wild-type TNF (wtTNF) (20 ng/ml; PeproTech), and M-CSF. Cells were then fixed and stained for tartrate-resistant acid phosphate (TRAP) according to the manufacturer's protocol (Cell Garage, Tokyo, Japan).

2.4. PEGylation of R1antTNF

R1antTNF in PBS was reacted with a 10-fold molar excess of mPEG-SPA 5000 (the succinimidyl ester of methoxy poly (ethylene glycol) propionic acid, average molecular weight 5,000; Shearwater, Huntsville, AL) against total primary amines of R1antTNF at 37 °C for 15 min, and then ε-amino caproic acid (10-fold molar excess against PEG) was added to stop the reaction. The reaction liquid was injected into gel filtration chromatography columns (Superose-12), and mono-PEGylated R1antTNF was collected. Collected samples were pooled, and run over Superose 12 columns again. Mono PEGylated R1antTNF was then separated, pooled again, and used as PEG–R1antTNF.

2.5. Surface plasmon resonance (SPR) assay

The binding kinetics of R1antTNF and PEG–R1antTNF were analyzed by the SPR technique using BIAcore 3000 (BIAcore®, GE Healthcare, Buckinghamshire, UK). Human TNFR1 (hTNFR1)-Fc chimera (R&D Systems, Minneapolis, MN) was diluted to 50 μg/ml in 10 mM sodium acetate buffer (pH 4.5). hTNFR1 was immobilized on a CM5 sensor chip, which resulted in an increase of 3,000–3,500 resonance units (RU). During the association phase, TNFs diluted in running buffer (HBS-EP) at 78.3, 26.1, 8.7 or 2.9 nM were individually passed over the immobilized hTNFR1 at a flow rate of 20 μl/min. During the dissociation phase, HBS-EP buffer was applied to the sensor chip at a flow rate of 20 μl/min. The data were analyzed globally with BIAEVALUATION 3.0 software (BIAcore®) using a 1:1 binding model.

2.6. Cytotoxicity assay

L-M cells (a mouse fibroblast cell line) were provided by Mochida Pharmaceutical Co Ltd (Tokyo, Japan) and maintained in MEM supplemented with 1% FBS and 1% antibiotic cocktail (Nacalai tesque, Kyoto, Japan). For the neutralization assay, a constant concentration of mouse wtTNF (5 ng/ml) and serial dilutions of R1antTNF were incubated with L-M cells (1×10^4 cells/well). After incubation for 48 h, cell survival was determined by methylene blue assays, as described previously [30].

2.7. Pharmacokinetic assay

Female BALB/c mice ($n = 5$) were injected i.p. with 100 μg R1antTNF or PEG–R1antTNF and blood samples drawn at different times thereafter. Serum concentrations of R1antTNF or PEG–R1antTNF were measured using an anti-human TNF ELISA kit (R&D Systems, Minneapolis, MN).

2.8. Induction of arthritis

Seven-week-old male DBA/1J mice were immunized by intradermal injection at the base of the tail with 100 μg of bovine type II collagen in 0.05 M acetic acid (Chondrex, Redmond, WA), emulsified in an equal volume of Freund's complete adjuvant (Chondrex). On day 21, mice received a type II collagen booster with an equal volume of incomplete Freund's adjuvant (Chondrex). For studies on prophylaxis, 3 μg PEG–R1antTNF or 25 μg Etanercept were administered i.p. twice daily or twice weekly, respectively, for 3 weeks starting at day 23. For therapy of established disease, administration of PBS, PEG–R1antTNF or Etanercept was started at day 28 when the average arthritis index was 0.5–1. Clinical arthritis was assessed by inspection every day, and inflammation of the 4 paws was graded from 0 to 4 as follows: grade 0, no swelling and focal redness; grade 1, swelling of finger joints; grade 2, slight swelling of ankle or wrist joints; grade 3, severe inflammation of the entire paw; and grade 4, deformity or ankylosis. Each paw was graded and the 4 scores were totaled so that the maximum possible score per mouse was 16. Blood was collected on day 50 after challenge, and serum IL-1β concentrations were measured by ELISA (R&D Systems).

2.9. Histology

The hind paws of each mouse were removed on day 43. One was fixed in 10% neutral buffered formalin, and decalcified with EDTA, embedded in paraffin, sectioned, and stained with hematoxylin–eosin. Radiographs were taken of the other hind paw. Serial sections were scored by investigators without knowledge of the experimental group. Destruction of ankle joint was scored as previously described [31,32] with modification. Cell filtration, synovitis, destruction of cartilage, and juxta-articular bone involvement were graded from 0 to 3. Each hind paw was graded and scores for the two paws were totaled so that the maximum possible score per mouse was 6.

2.10. Liver clearance of adenovirus

Recombinant fiber-modified adenovirus vector, containing an RGD (Arg-Gly-Asp) peptide in the fiber knob, and encoding the luciferase gene (Ad-Luc) was kindly provided by Dr. H. Mizuguchi (National Institute of Biomedical Innovation, Osaka, Japan). C57BL/6 mice (6 week-old females) were intravenously injected with Ad-Luc (5×10^9 PFU/mouse). The administration of PEG–R1antTNF and Etanercept was

started 1 day before Ad-Luc injection, and continued in a similar manner to the CIA model. One week after Ad-Luc injection, the mice were sacrificed and luciferase activity was measured as previously described [33].

2.11. Statistics

Mean values ± SD or SEM were compared by unpaired Student's *t*-test for parametric analysis. The mean arthritis index in each treatment group was compared using the Mann–Whitney *U* test. Statistical differences in arthritis incidence were determined by χ^2-test.

3. Results

3.1. Inhibitory effect of R1antTNF on osteoclast differentiation in vitro

Osteoclasts play an important role in bone resorption and are also involved in the progression of osteoporosis and arthritis. TNF is recognized as a potent inducer of osteoclastic differentiation [34]. It is mainly the interaction of TNF and TNFR1 which induces this osteoclastogenesis [35]. Previously, we reported that R1antTNF inhibited TNFR1-mediated functions, such as cytotoxicity, cytokine production, and NF-κB activation in some cell-lines, but whether it also inhibits TNF-induced osteoclast differentiation was not tested. Therefore, the inhibitory activity of R1antTNF on osteoclastogenesis was assessed on osteoclast progenitors derived from mouse bone marrow cells, which more accurately reflects the pathology than using cell-lines. Osteoclast progenitors derived from mouse bone marrow cells were incubated with mouse wild-type TNF (wtTNF) and R1antTNF, and the level of expression of tartrate-resistant acid phosphatase (TRAP), a marker of TNF-induced differentiation of osteoclasts, was measured. A 50-fold excess R1antTNF over wtTNF significantly decreased the number of TRAP-positive cells (Fig. 1a) and a 500-fold excess almost completely inhibited osteoclast differentiation (Fig. 1b). These results indicate that the R1antTNF is inhibitory for osteoclast differentiation.

3.2. In vivo stability and inhibitory activity of PEG–R1antTNF

To extend the half-life of R1antTNF in plasma, we applied our site-specific PEGylation to R1antTNF. While conventional PEGylation of TNF caused a loss of bioactivity due to random introduction of PEG at the ε-amino groups of six lysine residues in monomer TNF, our site-specific PEGylation introduces PEG only at the NH_2 terminus *via* lysine-deficient mutant TNF without loss of bioactivity. R1antTNF was generated using a phage library based on this lysine-deficient mutant TNF whereby R1antTNF is also lysine-deficient [25]. Because R1antTNF also forms homotrimers like wtTNF, PEGylated R1antTNFs containing one, two, or three PEG molecules could theoretically be created *via* the three N-termini of R1antTNF. Indeed, di-PEGylated, mono-PEGylated, and non-PEGylated R1antTNF were eluted in three peaks in that order by gel filtration chromatography (data not shown). We have previously reported that mono-PEGylated wtTNF retained complete bioactivity with superior *in vivo* stability compared to non-PEGylated TNF [28]. Therefore, mono-PEGylated R1antTNF was isolated, and assessed by SDS-PAGE analysis. Two bands, consisting of mono-PEGylated R1antTNF monomer and non-PEGylated R1antTNF monomer, were detected (data not shown), indicating that only one PEG molecule was introduced to one R1antTNF trimer molecule. This mono-PEGylated R1antTNF (PEG–R1antTNF) was used for the following study.

We next compared the binding affinity of PEG–R1antTNF and non-PEGylated R1antTNF for TNFR1 by SPR analysis, and the inhibitory activity on wtTNF-induced cytotoxicity against L-M cells,

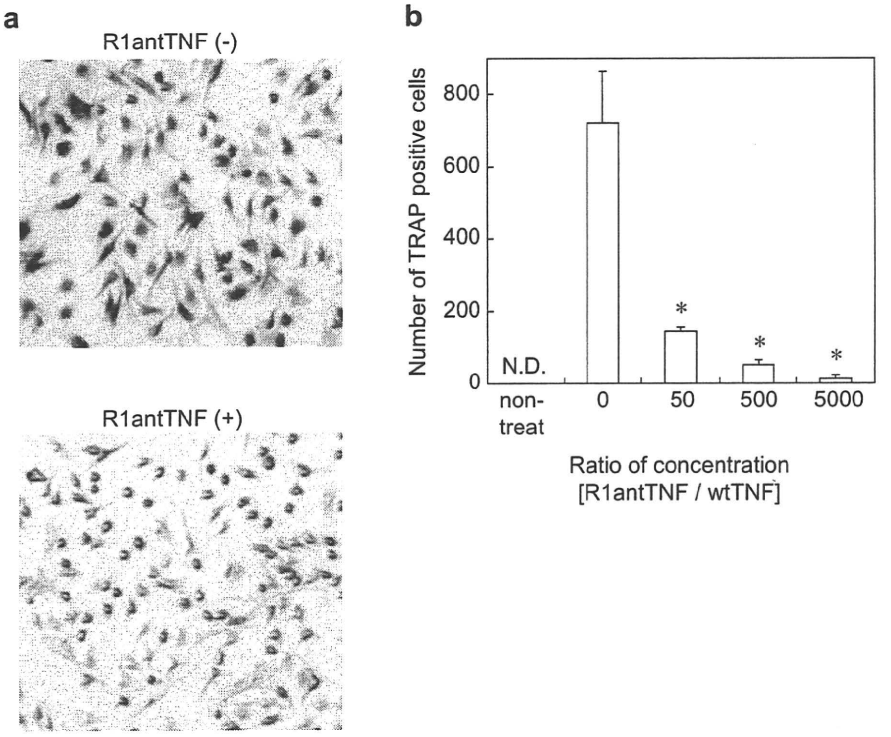

Fig. 1. Inhibitory effect of R1antTNF on TNF-mediated osteoclastogenesis. Bone marrow cells were incubated for 3 days with M-CSF, and adherent cells were stimulated with mouse wtTNF (20 ng/ml) in the presence of M-CSF with or without R1antTNF. After 5 days, cells were stained for TRAP (a) and the number of TRAP-positive cells was scored microscopically (b) ($n = 3$). The ratio of R1antTNF/wtTNF (+) is 50 in the photomicrograph of R1antTNF (a). *$p < 0.05$ versus non-treated.

a cell-line derived from L929 cells. The binding affinity of PEG–R1antTNF for TNFR1 was almost equivalent to that of R1antTNF (Fig. 2a). Additionally, PEG–R1antTNF inhibited wtTNF-induced cytotoxicity with the same efficiency as R1antTNF (Fig. 2b). To compare their *in vivo* stability, PEG–R1antTNF and R1antTNF were intraperitoneally injected into mice, and serum levels were measured at the indicated time points. In animals administered R1antTNF, the serum concentration was almost at the limit of detection 24 h after i.p. injection (Fig. 3). In contrast, the retention time of PEG–R1antTNF in the circulation was considerably longer than R1antTNF. These results suggest that mono-PEGylation markedly increases the *in vivo* stability of R1antTNF without decreasing its affinity for TNFR1 or its inhibitory activity.

3.3. PEG–R1antTNF treatment in the CIA model

We next investigated the protective effects of R1antTNF and PEG–R1antTNF against collagen-induced arthritis (CIA) in a mouse model. CIA is a chronic autoimmune model of human RA that is widely used for dissecting molecular and cellular mediators of this disease, as well as for evaluating possible therapeutic agents. Mice were treated with R1antTNF or PEG–R1antTNF at 3 μg or 1 μg/mouse twice a day for 3 weeks. We designed this dose schedule based on the retention time in the circulation and the endogenous

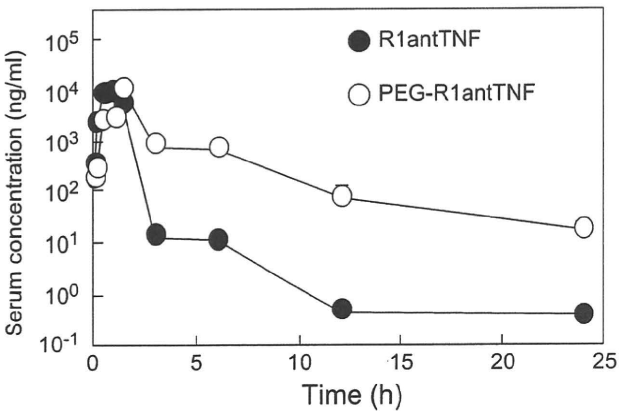

Fig. 3. Plasma levels of R1antTNF or PEG–R1antTNF after i.p. injection. 100 μg R1antTNF or PEG–R1antTNF was i.p. injected into mice ($n = 5$), and blood samples were collected at the indicated time points. The concentration of R1antTNF or PEG–R1antTNF in plasma was determined by ELISA. A standard curve was made for each R1antTNFs. Data represent the mean ± SD.

TNF levels in serum reported previously [36]. The treatment was started 2 days after the second immunization. In the PBS-treated group, the clinical score increased on day 26, and severe swelling of

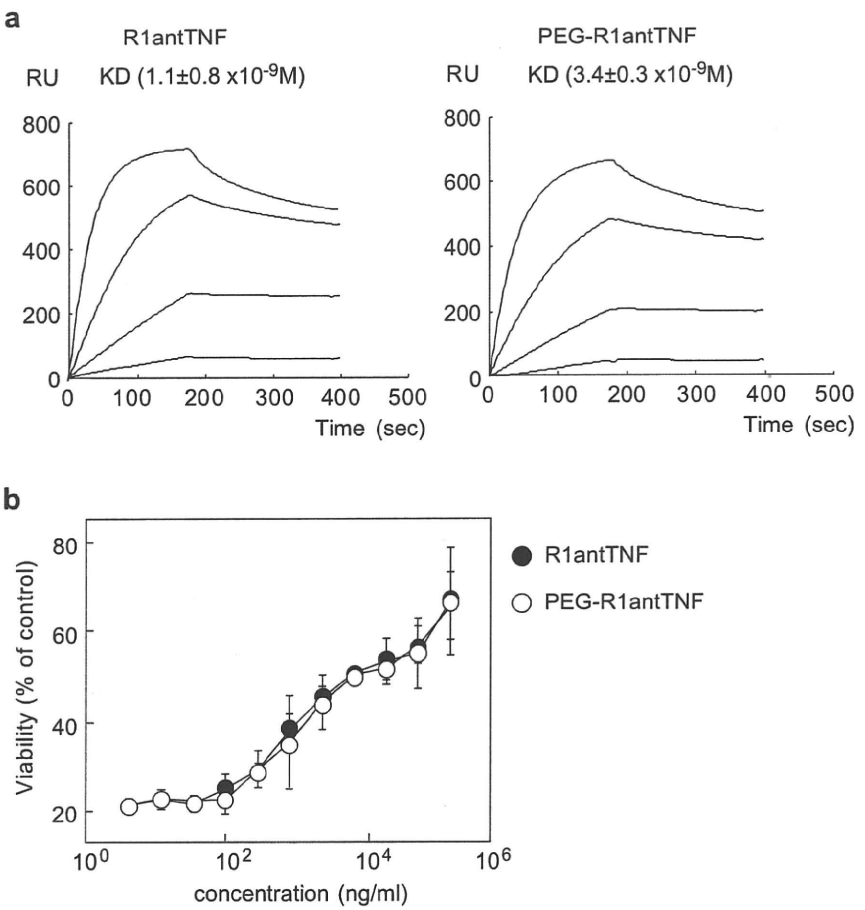

Fig. 2. Binding affinity and inhibitory activity of R1antTNF and PEG–R1antTNF. (a) Binding affinity of R1antTNF and PEG–R1antTNF was analyzed using the surface plasmon resonance (SPR) technique. TNFR1 was immobilized on a sensor chip CM5, which resulted in an increase of 3,000–3,500 resonance units (RU). The amount of protein bound to the surface was recorded in RU. Duplicate injections of 78.3, 26.1, 8.7 or 2.9 nM R1antTNF or PEG–R1antTNF were passed over the immobilized TNFR1 at a flow rate of 20 μl/min. The sensorgrams shown were normalized by subtracting the control surface sensorgram. (b) Serially diluted R1antTNF or PEG–R1antTNF was mixed with mouse wtTNF (5 ng/ml), and applied to L-M cells. After 48 h, the inhibitory activity on TNF-mediated cytotoxicity was assessed by the methylene blue assay ($n = 3$). The data represent the mean ± SD.

all four limbs was observed from around day 30 (Fig. 4). In the R1antTNF-treated groups, administration at 3 μg/mouse reduced the severity of arthritis, but administration at 1 μg/mouse had no effect (Fig. 4a). In contrast, in the PEG–R1antTNF-treated groups, administration of either 1 μg or 3 μg/mouse significantly decreased the severity of arthritis (Fig. 4b). In particular, while the severity of arthritis in the R1antTNF (1 μg/mouse)-treated group was almost the same as in the controls, treatment with PEG–R1antTNF at (1 μg/mouse) significantly suppressed the elevation of the arthritis score. In addition, treatment with PEG–R1antTNF at 1 μg/mouse delayed disease onset more noticeably than R1antTNF, indicating that the former has a superior inhibitory effect (Fig. 4c and d). Furthermore, treatment with PEG–R1antTNF at 3 μg/mouse significantly decreased the incidence of arthritis (Fig. 4d).

Next, to examine the effects of PEG–R1antTNF on pathology of ankle joints, we graded signs, such as bone destruction and cell infiltration, on sections (Table 1). Fig. 5 shows a typical example of an H&E-stained section and radiograph in each treatment group. While the joints of PEG–R1antTNF-treated mice exhibited much less inflammatory cell infiltration but only a trend toward reduction in synovitis, this agent did significantly prevent destruction of cartilage and bone involvement. This partially correlated with the inhibition of osteoclastogenesis mediated by R1antTNF *in vitro*. These results indicate that (1) R1antTNF has anti-inflammatory effects in the CIA model, and may prevent arthritis, (2) the application of our PEGylation strategy to R1antTNF enhanced this preventive effect probably due to improvement of *in vivo* stability without loss of inhibitory activity.

Table 1
Effect of PEG–R1antTNF on ankle joint pathology.

Treatment	Cell filtration	Synovitis	Destruction of cartilage	Juxta-articular bone involvement
Control (PBS)	3.71 ± 1.38	3.86 ± 1.07	2.00 ± 1.29	2.86 ± 1.22
PEG–R1antTNF				
1 μg/mouse	2.25 ± 1.99	2.25 ± 0.97$^{\#}$	0.38 ± 0.48$^{\#\#}$	0.63 ± 1.11$^{\#\#}$
3 μg/mouse	2.75 ± 0.89	2.63 ± 0.74$^{\#}$	0.88 ± 0.99	0.88 ± 0.99$^{\#\#}$

Data represent the mean ± SEM. $^{\#}p < 0.05$, $^{\#\#}p < 0.01$ verses Control (PBS) by Mann–Whitney *U* test.

3.4. Efficacy of PEG–R1antTNF compared to other agents for TNF blockade in the CIA model

We compared the effect of PEG–R1antTNF with Etanercept, an existing anti-TNF drug based on soluble TNFR2 fusion proteins in a prophylactic protocol similar to the above. Etanercept was administered at 25 μg/mouse twice a week for 3 weeks in accordance with reports of animal experiments in the package insert. PEG–R1antTNF was administered at 3 μg/mouse twice a day for 3 weeks, as described in the previous section. The plasma half-life of Etanercept is very long (about 90 h) due to its neonatal Fc receptor recycling, whereas the serum concentration of even PEG–R1antTNF 12 h after injection is only about one hundredth of its

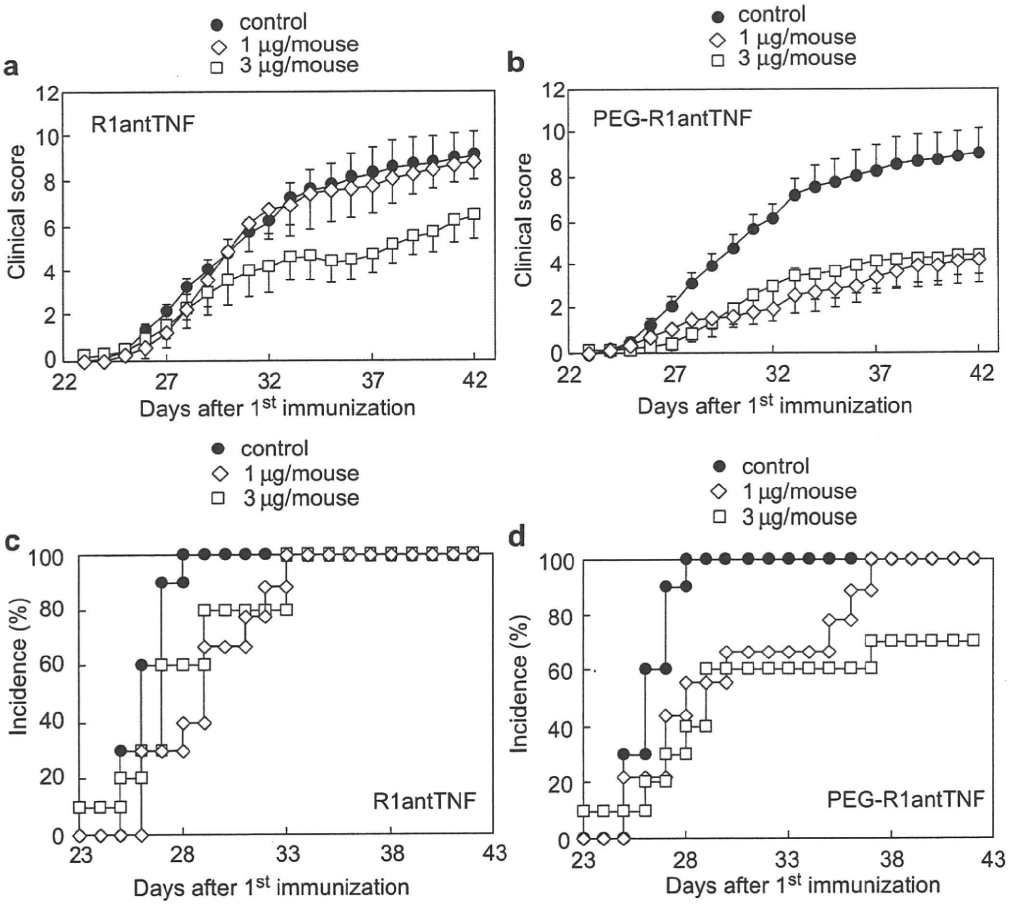

Fig. 4. Clinical score of CIA mice treated with R1antTNF or PEG–R1antTNF. The severity (a and b) and incidence (c and d) of arthritis in CIA mice ($n = 10$) treated with PBS, R1antTNF (1 or 3 μg twice a day) (a, c), or PEG–R1antTNF (1 or 3 μg twice a day) (b, d) for three weeks from 23 day was assessed every day using an established macroscopic scoring system. Data of severity represent the mean ± SEM. Incidence of arthritis represent the percentage of mice that developed CIA (clinical score ≥0.5).

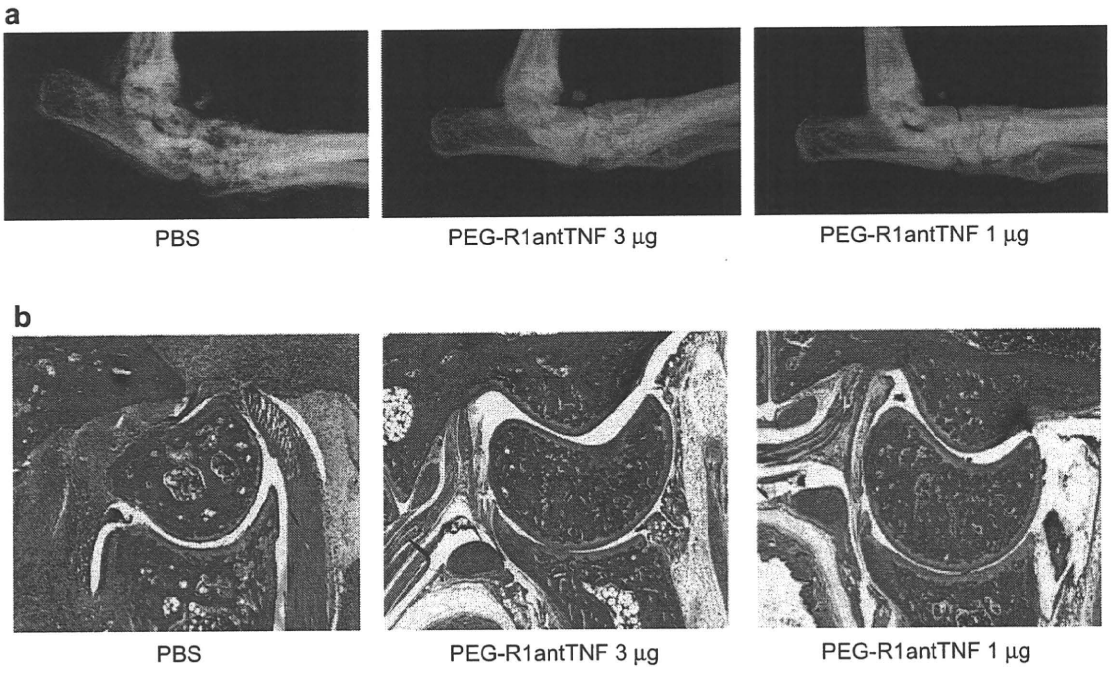

Fig. 5. Effect of PEG–R1antTNF on joint arthritis of hind paws. Macroradiographs of hind paws were taken on day 43 (a). H&E-stained sections of each CIA joint of the hind paws were also made on day 43 (b).

Cmax. Treatment with PEG–R1antTNF significantly reduced the severity of arthritis compared with the control group (Fig. 6a). While Etanercept completely inhibited arthritis up to day 33, at day 37 the arthritis score in the Etanercept-treated group was little different from the PEG–R1antTNF-treated group. Etanercept also decreased the incidence of arthritis and serum IL-1β levels more effectively than PEG–R1antTNF (Fig. 6b and c). Therefore, despite the findings that the effects of PEG–R1antTNF on the incidence of arthritis and serum IL-1β levels were less marked than those of Etanercept, the therapeutic activity of the former on disease severity was almost identical. No apparent toxicity was caused by PEG–R1antTNF and Etanercept after 3 weeks of continuous administration and the body weight of the treated mice was the same as controls (Fig. 6d). For clinical application, it is of course important to know whether the candidate drug exhibits therapeutic effects also on well-developed or extensively progressed arthritis. Therefore, we next examined the effect of PEG–R1antTNF on progression of established arthritis. Mice were treated with PEG–R1antTNF or Etanercept on day 28, when the average arthritis index was about 1.0. Treatment with PEG–R1antTNF significantly decreased the severity of disease (Fig. 7). These results indicate that not only prophylactic but also semi-therapeutic application of PEG–R1antTNF is effective in the CIA model.

3.5. Effect of PEG–R1antTNF on immunity to infection

A previous study using TNFR1- or TNFR2-deficient mice had indicated that TNF/TNFR2 interactions play an important role in antiviral-immune responses [37]. Therefore, we hypothesized that because it inhibits the bioactivity resulting from the interaction between TNF and TNFR1 but not between TNF and TNFR2, PEG–R1antTNF might not have the undesirable side effect of inhibiting antiviral immunity. Accordingly, we compared the effects of PEG–R1antTNF and Etanercept on antiviral immunity using a recombinant adenovirus vector, Ad-Luc. The administration of Etanercept and PEG–R1antTNF was started one day before Ad-Luc injection and continued as described for the CIA experiment. In the Etanercept-treated group, luciferase activity was significantly higher than in the control group, suggesting that the drug delayed clearance of the virus (Fig. 8). In contrast, luciferase activity of the PEG–R1antTNF-treated group was equivalent to controls, indicating that this agent was not detrimental for viral clearance. Thus, because of its TNFR1 selectivity, use of PEG–R1antTNF might avoid one of the concerns associated with potential side effects of anti-TNF blockers.

4. Discussion

In this study, we have investigated anti-inflammatory effects of a TNFR1-selective antagonistic mutant TNF (R1antTNF) in an animal model of RA. We showed that PEGylation of R1antTNF greatly improves its ability to suppress arthritis. This could be due to enhanced retention of R1antTNF in the circulating blood. Although the detailed pharmacokinetics of PEG–R1antTNF and R1antTNF still need to be analyzed, prolonged retention might increase the availability of R1antTNF to block TNF/TNFR1 interactions in the general circulation or lesion area, resulting in improved inhibitory activity. The reason for prolonged retention is believed to be that PEG moves very flexibly and forms an extensive hydrated layer on the surface of R1antTNF, causing a reduction of renal excretion due to increased apparent molecular weight and avoidance of attack by proteases. In this study, R1antTNF was conjugated to linear PEG5k, which is widely used for PEGylation of proteins, as a first approach. This was because we previously reported that when TNFs conjugated with four kinds of PEG (linear PEG5k, 20k, branched PEG10k, and 40k) were injected into tumor-bearing mice, the antitumor effect of PEG5k-TNF was almost equivalent to that of PEG10k-TNF and PEG20k-TNF, but PEG40k-TNF did not show any antitumor effects. However, for maximizing

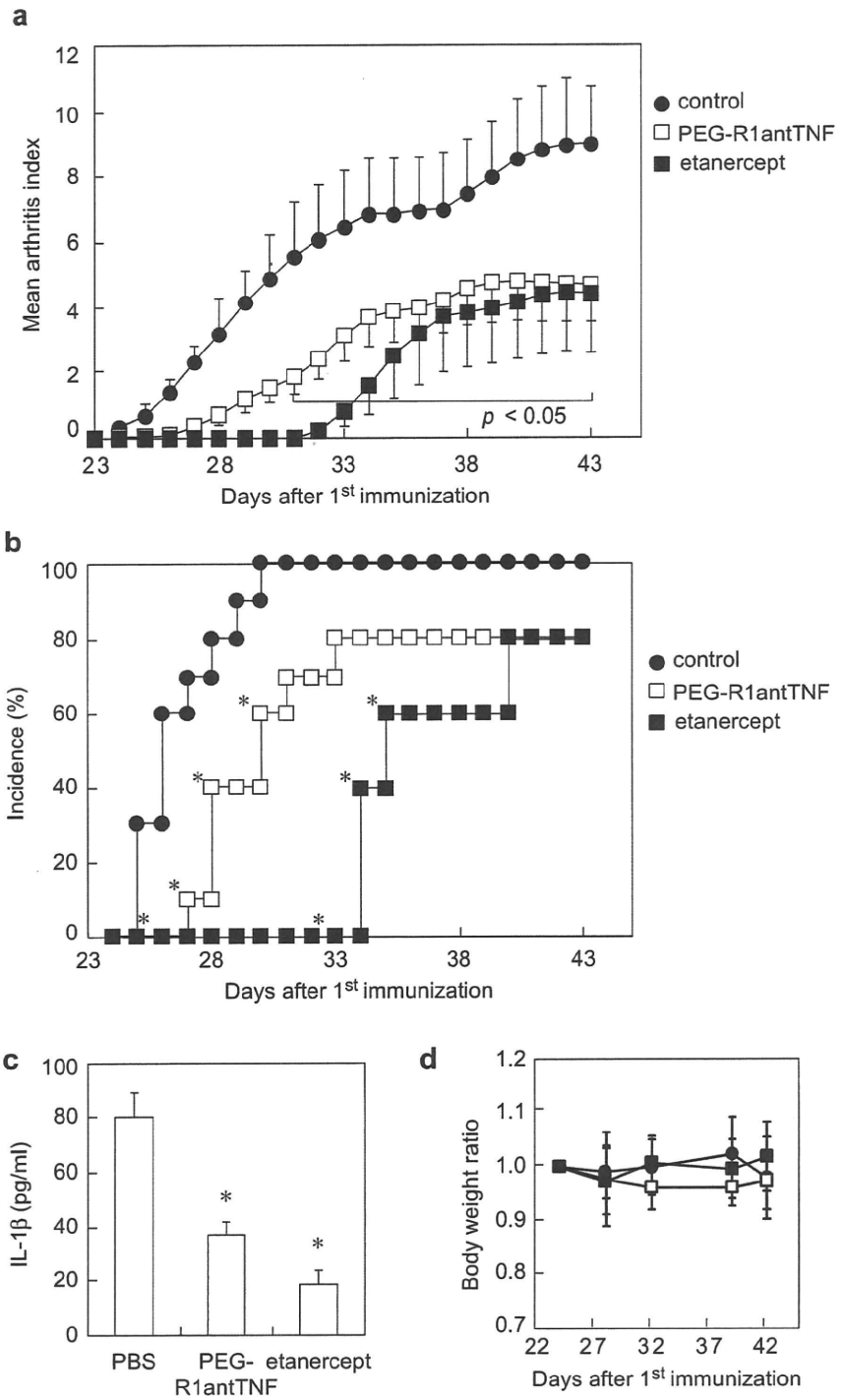

Fig. 6. Inhibitory effect of PEG–R1antTNF and Etanercept on CIA in mice. The severity (a) and incidence (b) of arthritis in CIA mice ($n = 8$) treated with PBS, PEG–R1antTNF (3 μg twice a day), or Etanercept (25 μg three times per week instead of twice a week) for three weeks from 23 day was assessed daily using an established macroscopic scoring system. Data represent the mean ± SEM. Serum concentration of IL-1β was determined by ELISA 43 days after the first immunization (c). *$p < 0.05$ versus PBS group. Body weight of CIA mice was measured 43 days after the first immunization (d).

the effectiveness of PEGylation, it is important to select the optimal molecular weight or type of PEG, balancing favorable effects, side effects, and dose schedule. Thus, selection of the optimal PEG for the treatment of arthritis or other chronic inflammatory diseases remains to be determined.

We found that prophylactically selectively blocking TNFR1 signaling by PEG–R1antTNF decreased the development and reduced the severity of arthritis. However, once arthritis became established in a joint, the symptoms were as severe as in the PBS treatment group (data not shown). Similar findings had already

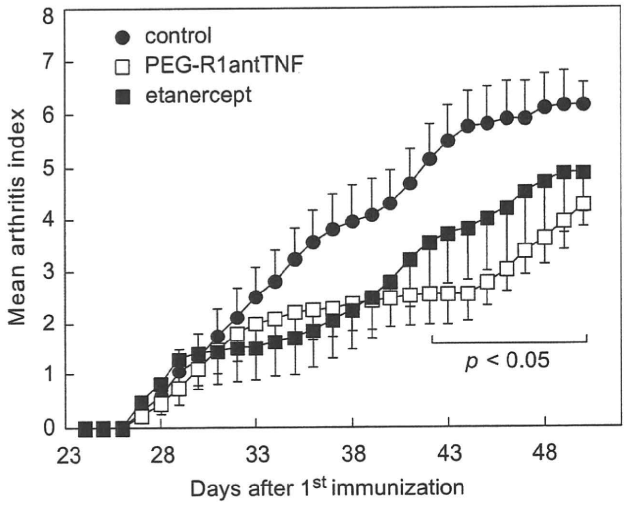

Fig. 7. Effect of PEG–R1antTNF and Etanercept on established arthritis in a semi-therapeutic protocol. The severity of arthritis in CIA mice ($n = 10$) treated with PBS, PEG–R1antTNF (3 μg twice a day), or Etanercept (25 μg three times per week instead of twice a week) for three weeks was assessed daily. $p < 0.05$ versus PBS group.

been noted in a previous study [15]. Thus, although in TNFR1 +/− mice the incidence and severity of arthritis were very low and mild respectively, once arthritis had developed, symptoms were as severe as in wild-type mice [15]. While it is possible that the inhibitory activity of PEG–R1antTNF is insufficient for complete suppression of arthritis, it also remains possible that there are many other factors in addition to TNF/TNFR1, which influence the development of arthritis. For example, IL-1 and IL-6 are known to be major arthritogenic cytokines in addition to TNF [3,38]. More recently, Cathepsin-K and Cadherin-11 were also reported to be

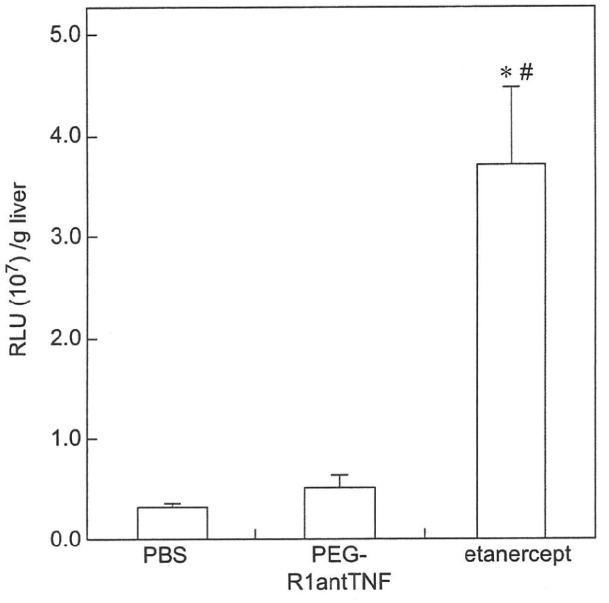

Fig. 8. Influence of PEG–R1antTNF and Etanercept on clearance of adenovirus from the liver. Mice were infected with Ad-Luc, and luciferase expression in the liver was assessed 7 days after infection. Administration of PEG–R1antTNF or Etanercept was started 1 day before infection, and continued as described for the experiments in CIA mice. RLU, relative light units. $^{*}p < 0.05$ versus PBS group. $^{\#}p < 0.05$ versus PEG–R1antTNF group.

involved in the autoimmune inflammation of arthritis, in a manner unrelated to TNF-associated cytokine cascades [39,40]. Therefore, a combination of PEG–R1antTNF with inhibitors of these molecules might prevent arthritis more efficiently than a single agent.

In contrast to the prophylactic model, comparison of PEG–R1antTNF and Etanercept in a semi-therapeutic protocol demonstrated that the former was significantly effective, with the latter showing only a tendency to reduce the arthritis index. This is consistent with the consensus that existing TNF inhibitors do not show great efficacy once arthritis and swelling have already become severe in CIA model. Previous studies reported that in established CIA model anti-TNF antibody had no significant effect on cartilage or bone destruction, although IL-1 blockade prevented cartilage and bone destruction [31,41]. However, it's an undisputable fact clinical treatment using TNF blockade in RA patients showed suppression of joint destruction. Because mechanisms responsible for the therapeutic effects of Etanercept on CIA are not well-investigated, the exact reasons for this result are not clear. According to the product package insert, the clinical dose of Etanercept is 25 mg/body (about 400 μg/kg) twice per week, and the effective dose in the murine CIA model is 1–150 μg/body (about 50 to 7500 μg/kg). Thus, the dose of Etanercept used in our study seems to be within the effective range. Another possible explanation for the effectiveness of PEG–R1antTNF is its potential to inhibit only TNFR1, whereas both TNFR1 and TNFR2 are blocked by Etanercept. While the role of TNFR2 in RA models is still less well understood, Tada et al. showed that the repeated administration of murine TNF to TNFR1-knockout mice after the onset of symptoms did reduce arthritis, but enhanced it during the early inflammatory phase, suggesting that TNFR2 plays a dual opposing role in CIA in a stage-dependent manner, and illustrating an immunosuppressive effect of TNF [42], which we wanted to exploit in our TNFR1-directed strategy. In addition, TNFR2-deficient mice exhibited an exacerbated TNFR1-dependent pulmonary inflammatory response, suggesting a dominant role for endogenous TNFR2 in attenuating leukocyte accumulation within the lung [43]. Interestingly, a recent report indicated that the TNF/TNFR2 interaction accelerates the expansion of $CD4^{+}$ and $CD25^{+}$ T regulatory cells, suggesting that TNF might induce immunosuppressive effects *via* TNFR2 expressed on T regulatory cells [44]. Therefore, in a semi-therapeutic protocol, it might be possible that PEG–R1antTNF exerts a significant effect in the murine CIA model due to its TNFR1 selectivity, contrasting with the blocking of TNFR2 as well as TNFR1 signaling by Etanercept. Our data thus demonstrate that the selective inhibition of TNFR1 could be effective when in treating established arthritis.

The complete suppression of TNF, which plays a critical role in many immune functions, can disrupt host defense systems, resulting in infectious diseases; indeed, tuberculosis and bacterial infection are known to be increased under TNF blockade [45]. In addition, the risk of exacerbation or reactivation of viral hepatitis type B by TNF blockade has also recently been flagged [13,46]. The relative importance of TNFR2 rather than TNFR1 for host defense against viruses has been proposed [37,47]. In the present study, we investigated the effect of Etanercept and PEG–R1antTNF on viral immunity, using adenovirus infection as a model. While viral clearance was indeed compromised by the administration of Etanercept, PEG–R1antTNF had little effect on this important parameter. This indicated that use of PEG–R1antTNF may reduce side effects such as increased susceptibility to viral infection due to its TNFR1 selectivity. On the other hand, tmTNF, a dominant ligand of TNFR2, is believed to maintain resistance to tuberculosis or other bacterial infections in the absence of soluble TNF [22,23]. Recently, several studies have shown that selective inhibitors of soluble TNF, which cannot block the activity of tmTNF, nonetheless protect against arthritis without suppression of immunity to infection

[48,49]. Because PEG–R1antTNF does not bind TNFR2, PEG–R1antTNF cannot inhibit the interaction of tmTNF with TNFR2. Therefore, it might be that PEG–R1antTNF would also have reduced side effects in the context of bacterial infection as well.

5. Conclusions

Our studies reported here demonstrated that the TNFR1-selective blocking strategy is effective for the treatment of RA, using a TNFR1-selective antagonistic mutant TNF. Furthermore, our site-specific PEGylation technique described here can enhance the therapeutic effect of R1antTNF. We are now planning to develop this drug-delivery carrier approach for further improvement of *in vivo* stability and to apply R1antTNF in gene therapy.

Acknowledgment

The authors thank Dr. Peter Vandenabeele (Department of Molecular Biology, Gent University) and Dr. Bharat B. Aggarwal (Department of Experimental Therapeutics, The University of Texas M.D. Anderson Cancer Center) for their helpful discussions. This study was supported in part by Grants-in-Aid for Scientific Research from the Ministry of Education, Culture, Sports, Science and Technology of Japan, and from the Japan Society for the Promotion of Science (JSPS). This study was also supported in part by Health Labour Sciences Research Grants from the Ministry of Health, Labor and Welfare of Japan; by Health Sciences Research Grants for Research on Publicly Essential Drugs and Medical Devices from the Japan Health Sciences Foundation; by a Grant from Minister of the Environment; and by The Nagai Foundation Tokyo.

Appendix

Figures with essential color discrimination. Figs. 1 and 5 of this article are difficult to interpret in black and white. The full color images can be found in the on-line version, at doi:10.1016/j.biomaterials.2009.08.041.

References

[1] Lee DM, Weinblatt ME. Rheumatoid arthritis. Lancet 2001 Sep 15;358(9285):903–11.
[2] Chu CQ, Field M, Feldmann M, Maini RN. Localization of tumor necrosis factor alpha in synovial tissues and at the cartilage–pannus junction in patients with rheumatoid arthritis. Arthritis Rheum 1991 Sep;34(9):1125–32.
[3] Feldmann M, Brennan FM, Maini RN. Rheumatoid arthritis. Cell 1996 May 3;85(3):307–10.
[4] Maury CP, Teppo AM. Cachectin/tumour necrosis factor-alpha in the circulation of patients with rheumatic disease. Int J Tissue React 1989;11(4):189–93.
[5] Feldmann M, Maini RN. Lasker Clinical Medical Research Award. TNF defined as a therapeutic target for rheumatoid arthritis and other autoimmune diseases. Nat Med 2003 Oct;9(10):1245–50.
[6] Thorbecke GJ, Shah R, Leu CH, Kuruvilla AP, Hardison AM, Palladino MA. Involvement of endogenous tumor necrosis factor alpha and transforming growth factor beta during induction of collagen type II arthritis in mice. Proc Natl Acad Sci U S A 1992 Aug 15;89(16):7375–9.
[7] Williams RO, Feldmann M, Maini RN. Anti-tumor necrosis factor ameliorates joint disease in murine collagen-induced arthritis. Proc Natl Acad Sci U S A 1992 Oct 15;89(20):9784–8.
[8] Moreland LW, Schiff MH, Baumgartner SW, Tindall EA, Fleischmann RM, Bulpitt KJ, et al. Etanercept therapy in rheumatoid arthritis. A randomized, controlled trial. Ann Intern Med 1999 Mar 16;130(6):478–86.
[9] Chung ES, Packer M, Lo KH, Fasanmade AA, Willerson JT. Randomized, double-blind, placebo-controlled, pilot trial of infliximab, a chimeric monoclonal antibody to tumor necrosis factor-alpha, in patients with moderate-to-severe heart failure: results of the anti-TNF Therapy Against Congestive Heart Failure (ATTACH) trial. Circulation 2003 Jul 1;107(25):3133–40.
[10] Mohan N, Edwards ET, Cupps TR, Oliverio PJ, Sandberg G, Crayton H, et al. Demyelination occurring during anti-tumor necrosis factor alpha therapy for inflammatory arthritides. Arthritis Rheum 2001 Dec;44(12):2862–9.
[11] Shakoor N, Michalska M, Harris CA, Block JA. Drug-induced systemic lupus erythematosus associated with etanercept therapy. Lancet 2002 Feb 16;359(9306):579–80.
[12] Gomez-Reino JJ, Carmona L, Valverde VR, Mola EM, Montero MD. Treatment of rheumatoid arthritis with tumor necrosis factor inhibitors may predispose to significant increase in tuberculosis risk: a multicenter active-surveillance report. Arthritis Rheum 2003 Aug;48(8):2122–7.
[13] Lubel JS, Testro AG, Angus PW. Hepatitis B virus reactivation following immunosuppressive therapy: guidelines for prevention and management. Intern Med J 2007 Oct;37(10):705–12.
[14] Brown SL, Greene MH, Gershon SK, Edwards ET, Braun MM. Tumor necrosis factor antagonist therapy and lymphoma development: twenty-six cases reported to the Food and Drug Administration. Arthritis Rheum 2002 Dec;46(12):3151–8.
[15] Mori L, Iselin S, De Libero G, Lesslauer W. Attenuation of collagen-induced arthritis in 55-kDa TNF receptor type 1 (TNFR1)-IgG1-treated and TNFR1-deficient mice. J Immunol 1996 Oct 1;157(7):3178–82.
[16] Butler DM, Malfait AM, Mason LJ, Warden PJ, Kollias G, Maini RN, et al. DBA/1 mice expressing the human TNF-alpha transgene develop a severe, erosive arthritis: characterization of the cytokine cascade and cellular composition. J Immunol 1997 Sep 15;159(6):2867–76.
[17] Keffer J, Probert L, Cazlaris H, Georgopoulos S, Kaslaris E, Kioussis D, et al. Transgenic mice expressing human tumour necrosis factor: a predictive genetic model of arthritis. EMBO J 1991 Dec;10(13):4025–31.
[18] Kim EY, Priatel JJ, Teh SJ, Teh HS. TNF receptor type 2 (p75) functions as a costimulator for antigen-driven T cell responses in vivo. J Immunol 2006 Jan 15;176(2):1026–35.
[19] Kim EY, Teh HS. TNF type 2 receptor (p75) lowers the threshold of T cell activation. J Immunol 2001 Dec 15;167(12):6812–20.
[20] Grell M, Becke FM, Wajant H, Mannel DN, Scheurich P. TNF receptor type 2 mediates thymocyte proliferation independently of TNF receptor type 1. Eur J Immunol 1998 Jan;28(1):257–63.
[21] Grell M, Douni E, Wajant H, Lohden M, Clauss M, Maxeiner B, et al. The transmembrane form of tumor necrosis factor is the prime activating ligand of the 80 kDa tumor necrosis factor receptor. Cell 1995 Dec 1;83(5):793–802.
[22] Olleros ML, Guler R, Corazza N, Vesin D, Eugster HP, Marchal G, et al. Transmembrane TNF induces an efficient cell-mediated immunity and resistance to *Mycobacterium bovis* bacillus Calmette-Guerin infection in the absence of secreted TNF and lymphotoxin-alpha. J Immunol 2002 Apr 1;168(7):3394–401.
[23] Saunders BM, Tran S, Ruuls S, Sedgwick JD, Briscoe H, Britton WJ. Transmembrane TNF is sufficient to initiate cell migration and granuloma formation and provide acute, but not long-term, control of *Mycobacterium tuberculosis* infection. J Immunol 2005 Apr 15;174(8):4852–9.
[24] Kollias G, Kontoyiannis D. Role of TNF/TNFR in autoimmunity: specific TNF receptor blockade may be advantageous to anti-TNF treatments. Cytokine Growth Factor Rev 2002 Aug–Oct;13(4–5):315–21.
[25] Shibata H, Yoshioka Y, Ohkawa A, Minowa K, Mukai Y, Abe Y, et al. Creation and X-ray structure analysis of the tumor necrosis factor receptor-1-selective mutant of a tumor necrosis factor-alpha antagonist. J Biol Chem 2008 Jan 11;283(2):998–1007.
[26] Shibata H, Yoshioka Y, Ohkawa A, Abe Y, Nomura T, Mukai Y, et al. The therapeutic effect of TNFR1-selective antagonistic mutant TNF-alpha in murine hepatitis models. Cytokine 2008 Nov;44(2):229–33.
[27] Shibata H, Yoshioka Y, Ikemizu S, Kobayashi K, Yamamoto Y, Mukai Y, et al. Functionalization of tumor necrosis factor-alpha using phage display technique and PEGylation improves its antitumor therapeutic window. Clin Cancer Res 2004 Dec 15;10(24):8293–300.
[28] Yamamoto Y, Tsutsumi Y, Yoshioka Y, Nishibata T, Kobayashi K, Okamoto T, et al. Site-specific PEGylation of a lysine-deficient TNF-alpha with full bioactivity. Nat Biotechnol 2003 May;21(5):546–52.
[29] Yoshioka Y, Tsutsumi Y, Ikemizu S, Yamamoto Y, Shibata H, Nishibata T, et al. Optimal site-specific PEGylation of mutant TNF-alpha improves its antitumor potency. Biochem Biophys Res Commun 2004 Mar 19;315(4):808–14.
[30] Tsutsumi Y, Kihira T, Tsunoda S, Kanamori T, Nakagawa S, Mayumi T. Molecular design of hybrid tumour necrosis factor alpha with polyethylene glycol increases its anti-tumour potency. Br J Cancer 1995 May;71(5):963–8.
[31] Joosten LA, Helsen MM, van de Loo FA, van den Berg WB. Anticytokine treatment of established type II collagen-induced arthritis in DBA/1 mice. A comparative study using anti-TNF alpha, anti-IL-1 alpha/beta, and IL-1Ra. Arthritis Rheum 1996 May;39(5):797–809.
[32] Larsson E, Erlandsson Harris H, Larsson A, Mansson B, Saxne T, Klareskog L. Corticosteroid treatment of experimental arthritis retards cartilage destruction as determined by histology and serum COMP. Rheumatology (Oxford) 2004 Apr;43(4):428–34.
[33] Koizumi N, Kawabata K, Sakurai F, Watanabe Y, Hayakawa T, Mizuguchi H. Modified adenoviral vectors ablated for coxsackievirus–adenovirus receptor, alphav integrin, and heparan sulfate binding reduce in vivo tissue transduction and toxicity. Hum Gene Ther 2006 Mar;17(3):264–79.
[34] Redlich K, Hayer S, Ricci R, David JP, Tohidast-Akrad M, Kollias G, et al. Osteoclasts are essential for TNF-alpha-mediated joint destruction. J Clin Invest 2002 Nov;110(10):1419–27.
[35] Zhang YH, Heulsmann A, Tondravi MM, Mukherjee A, Abu-Amer Y. Tumor necrosis factor-alpha (TNF) stimulates RANKL-induced osteoclastogenesis via coupling of TNF type 1 receptor and RANK signaling pathways. J Biol Chem 2001 Jan 5;276(1):563–8.

[36] Zhou GQ, Zhao N, Zhang H, Jia HW, Zhang WD, Zhao LH, et al. Effect of Gui Zhi decoction on enteric mucosal immune in mice with collagen-induced arthritis. World J Gastroenterol 2005 Sep 14;11(34):5373–6.
[37] Kafrouni MI, Brown GR, Thiele DL. The role of TNF–TNFR2 interactions in generation of CTL responses and clearance of hepatic adenovirus infection. J Leukoc Biol 2003 Oct;74(4):564–71.
[38] Firestein GS. Evolving concepts of rheumatoid arthritis. Nature 2003 May 15;423(6937):356–61.
[39] Lee DM, Kiener HP, Agarwal SK, Noss EH, Watts GF, Chisaka O, et al. Cadherin-11 in synovial lining formation and pathology in arthritis. Science 2007 Feb 16;315(5814):1006–10.
[40] Asagiri M, Hirai T, Kunigami T, Kamano S, Gober HJ, Okamoto K, et al. Cathepsin K-dependent toll-like receptor 9 signaling revealed in experimental arthritis. Science 2008 Feb 1;319(5863):624–7.
[41] Joosten LA, Helsen MM, Saxne T, van De Loo FA, Heinegard D, van Den Berg WB. IL-1 alpha beta blockade prevents cartilage and bone destruction in murine type II collagen-induced arthritis, whereas TNF-alpha blockade only ameliorates joint inflammation. J Immunol 1999 Nov 1;163(9):5049–55.
[42] Tada Y, Ho A, Koarada S, Morito F, Ushiyama O, Suzuki N, et al. Collagen-induced arthritis in TNF receptor-1-deficient mice: TNF receptor-2 can modulate arthritis in the absence of TNF receptor-1. Clin Immunol 2001 Jun;99(3):325–33.
[43] Peschon JJ, Torrance DS, Stocking KL, Glaccum MB, Otten C, Willis CR, et al. TNF receptor-deficient mice reveal divergent roles for p55 and p75 in several models of inflammation. J Immunol 1998 Jan 15;160(2):943–52.
[44] Chen X, Baumel M, Mannel DN, Howard OM, Oppenheim JJ. Interaction of TNF with TNF receptor type 2 promotes expansion and function of mouse CD4 + CD25 + T regulatory cells. J Immunol 2007 Jul 1;179(1):154–61.
[45] Winthrop KL. Risk and prevention of tuberculosis and other serious opportunistic infections associated with the inhibition of tumor necrosis factor. Nat Clin Pract Rheumatol 2006 Nov;2(11):602–10.
[46] Nathan DM, Angus PW, Gibson PR. Hepatitis B and C virus infections and anti-tumor necrosis factor-alpha therapy: guidelines for clinical approach. J Gastroenterol Hepatol 2006 Sep;21(9):1366–71.
[47] Chan FK, Shisler J, Bixby JG, Felices M, Zheng L, Appel M, et al. A role for tumor necrosis factor receptor-2 and receptor-interacting protein in programmed necrosis and antiviral responses. J Biol Chem 2003 Dec 19;278(51):51613–21.
[48] Zalevsky J, Secher T, Ezhevsky SA, Janot L, Steed PM, O'Brien C, et al. Dominant-negative inhibitors of soluble TNF attenuate experimental arthritis without suppressing innate immunity to infection. J Immunol 2007 Aug 1;179(3):1872–83.
[49] Spohn G, Guler R, Johansen P, Keller I, Jacobs M, Beck M, et al. A virus-like particle-based vaccine selectively targeting soluble TNF-alpha protects from arthritis without inducing reactivation of latent tuberculosis. J Immunol 2007 Jun 1;178(11):7450–7.

National Institute of Biomedical Innovation (NiBio)[1]; Graduate School of Pharmaceutical Sciences[2], Osaka University; The Center for Advanced Medical Engineering and Informatics[3], Osaka University, Osaka, Japan

Creation of an improved mutant TNF with TNFR1-selectivity and antagonistic activity by phage display technology

T. NOMURA[1,2*], Y. ABE[1*], H. KAMADA[1,3], M. INOUE[1], T. KAWARA[1,2], S. ARITA[1,2], T. FURUYA[1,2], K. MINOWA[1], Y. YOSHIOKA[2,3], H. SHIBATA[1], H. KAYAMURO[1,2], T. YAMASHITA[1,2], K. NAGANO[1], T. YOSHIKAWA[1,2], Y. MUKAI[2], S. NAKAGAWA[2,3], S. TSUNODA[1,2,3], Y. TSUTSUMI[1,2,3]

Received August 7, 2009, accepted August 14, 2009

Shin-ichi Tsunoda, Ph.D., Laboratory of Pharmaceutical Proteomics, National Institute of Biomedical Innovation, 7-6-8 Saito-Asagi, Ibaraki, Osaka 567-0085, Japan
tsunoda@nibio.go.jp
**These authors contributed equally to the work.*

Pharmazie 65: 93–96 (2010) *doi: 10.1691/ph.2010.9265*

Tumor necrosis factor-α (TNF), which binds two types of TNF receptors (TNFR1 and TNFR2), regulates the onset and exacerbation of autoimmune diseases such as rheumatoid arthritis and Crohn's disease. In particular, TNFR1-mediated signals are predominantly related to the induction of inflammatory responses. We have previously generated a TNFR1-selective antagonistic TNF-mutant (mutTNF) and shown that mutTNF efficiently inhibits TNFR1-mediated bioactivity *in vitro* and attenuates inflammatory conditions *in vivo*. In this study, we aimed to improve the TNFR1-selectivity of mutTNF. This was achieved by constructing a phage library displaying mutTNF-based variants, in which the amino acid residues at the predicted receptor binding sites were substituted to other amino acids. From this mutant TNF library, 20 candidate TNFR1-selective antagonists were isolated. Like mutTNF, all 20 candidates were found to have an inhibitory effect on TNFR1-mediated bioactivity. However, one of the mutants, N7, displayed significantly more than 40-fold greater TNFR1-selectivty than mutTNF. Therefore, N7 could be a promising anti-autoimmune agent that does not interfere with TNFR2-mediated signaling pathways.

1. Introduction

The severity and progression of inflammatory diseases, such as rheumatoid arthritis, Crohn's disease and ulcerative colitis, can be correlated with the serum level of tumor necrosis factor-α (TNF). Thus, TNF blockades such as anti-TNF antibodies and soluble TNFRs, which neutralize the activity of TNF, have been used to treat various autoimmune diseases in clinical practice. However, TNF blockades inhibit both TNFR1 and TNFR2 signaling. Thus, treatment with these drugs can lead to an increased risk of infection (Gomez-Reino et al. 2003; Lubel et al. 2007) and lymphoma development (Brown et al. 2002). TNF has been reported to induce inflammatory response predominantly through TNFR1 (Mori et al. 1996), whereas activation of the immune response is initiated *via* TNFR2 (Kim et al. 2006; Kim and Teh 2001; Grell et al. 1998). Therefore, blocking TNFR1-signaling, but not TNFR2-signaling, is a promising strategy for the safe and effective treatment of inflammatory diseases, which overcomes the risk of infection associated with the use of non-specific TNF blockades (Kollias and Kontoyiannis 2002).

In our previous studies, we used the phage display technique (Imai et al. 2008; Nagano et al. 2009; Nomura et al. 2007) to generate a TNFR1-selective antagonistic mutant TNF (mutTNF) that blocks TNFR1-mediated signals but not those of TNFR2 (Shibata et al. 2008b). Moreover, mutTNF showed superior therapeutic effects using an inflammatory disease mouse model (Shibata et al. 2008a). Thus, a drug for autoimmune diseases that selectively targets TNFR1 is anticipated to display higher efficacy and safety compared to existing treatments. In this study, we have attempted to isolate TNFR1-selective antagonists with higher TNFR1-selectivity than previous mutTNF by constructing a modified phage library displaying mutTNF-based variants.

2. Investigations, results and discussion

Here, we attempted to improve the TNFR1-selectivity of mutTNF using a phage display technique. Firstly, we constructed a phage library of TNF mutant using mutTNF as template. We designed a randomized library of mutTNF to replace the six amino acid residues (aa 29, 31, 32, 145–147) in the predicted receptor binding site. As a result of the 2-step PCR, we confirmed that the mutTNF mutant library consisted of 4×10^7 independent recombinant clones (*data not shown*). To enrich for TNFR1-selective antagonists, the phage library was subjected to two rounds of panning against TNFR1 on a Biacore biosensor chip. After the second panning, supernatants of single clone of *E. coli* TG1 including phagemid were randomly collected and subjected to screening by bioassay and ELISA to evaluate their bioactivity and affinity against each TNF receptor, respectively (*data not shown*). Consequently, twenty candidates of TNFR1-selective mutants with antagonistic activity were isolated (Table).

Next, we determined the detailed biological properties of each candidate. Positive clones were engineered for expression in

Table: Amino acid sequences and biological properties of TNFR1-selective antagonist candidates

TNF	Amino acid sequence						Relative affinity (% K_d)[a]			Bioactivity via TNFR1	
	29	31	32	145	146	147	TNFR1	TNFR2	TNFR1[b]/TNCR2	Agonistic[c] activity	Antagonisti[d] activity
mutTNF	L	R	R	A	E	S	100.0	100.0	1.0	–	+
N1	S	–	W	R	–	–	550.0	21.6	25.5	+	–
N2	S	–	W	–	–	–	200.0	N.D.	N.D.	+	–
N3	S	–	W	R	D	–	550.0	44.8	12.3	–	±
N4	S	–	W	–	D	–	183.3	19.1	9.6	±	–
N5	S	–	W	–	S	E	275.0	25.8	10.7	±	–
N6	A	D	T	–	–	–	200.0	21.6	9.3	±	–
N7	S	N	D	D	A	–	104.7	2.5	41.9	–	+
N8	R	I	A	D	–	–	169.2	26.7	6.3	+	–
N9	H	H	–	–	N	G	169.2	33.0	5.1	+	–
N10	T	N	N	–	–	–	314.3	28.6	11.0	±	–
N11	T	N	N	S	–	–	275.0	18.3	15.0	±	–
N12	F	S	T	–	–	–	440.0	58.0	7.6	+	–
N13	F	S	T	–	S	E	440.0	73.9	6.0	+	–
N14	R	W	Y	T	N	T	314.3	19.2	16.4	+	–
N15	F	K	T	N	A	T	275.0	24.1	11.4	±	–
N16	M	L	T	N	S	T	367.0	7.7	47.7	+	–
N17	Y	L	A	T	H	T	137.5	1.6	86.0	±	–
N18	Y	L	A	T	H	–	110.0	4.7	23.4	±	–
N19	V	Q	Y	N	N	–	367.0	N.D.	N.D.	±	–
N20	F	S	T	P	Q	R	244.4	N.D.	N.D.	±	–

Conserved residues compared with mutTNF are indicated by an em dash (–) The affinity values are shown as relative values (% mutTNF). N.D.: not detected

[a] Affinity for immobilized TNFR1 and TNFR2 was assessed by SPR using BIAcore3000. The dissociation constant (K_d) of TNF mutants were calculated from their sensorgrams by BIAEVALUATION 4.0 software

[b] TNFR1-selectivity was defined as relative affinity [TNFE1]/ relative affinity [TNFR2] for mutTNF

[c] TNFR1-mediated agonistic activity was measured, using a HEp-2 cell cytotoxicity assay. The intensity in agonistic activity was evaluated as the following. Cell viability at 10^4 ng/ml each mutant. 0–25% (of non treatment); (+), 25–50%; (±), 50–100%; (–)

[d] TNFR1-mediated antagonistic activity of mutant TNFs on wtTNF induced cytotoxicity in HEp-2 cells was measured. The intensity in antagonistic activity was evaluated as the following. Cell viability at 10^5 ng/ml each mutant in present of 5 ng/ml wtTNF. 0–25% (of non treatment); (–), 25–50%; (±), 50–100%; (+)

E. coli BL21λDE3 and each recombinant protein was purified as described previously (Yamamoto 2003). As anticipated, gel electrophoresis confirmed the mutant TNF proteins to have a molecular weight of 17 kDa. Moreover, gel filtration chromatography established that each mutant forms a homotrimeric complex in solution, as is the case for wild-type TNF (wtTNF) (*data not shown*). To analyze the binding properties of these TNFR1-selective TNF candidates, their dissociation constants (K_d) for TNFR1 and TNFR2 were measured using a surface plasmon resonance (SPR) analyzer. Our previous SPR analysis showed that although mutTNF has an almost identical affinity to TNFR1 as to wtTNF, it displays more than 17,000-fold greater selectivity for TNFR1. As shown in the Table, all the candidates exhibited higher affinity for TNFR1 than mutTNF. Furthermore, clones N1, N7, N16, N17 and N18 showed more than 20-fold higher TNFR1-binding selectivity compared to mutTNF. To examine the bioactivity of all candidates *via* TNFR1, we subsequently performed a cytotoxicity assay using

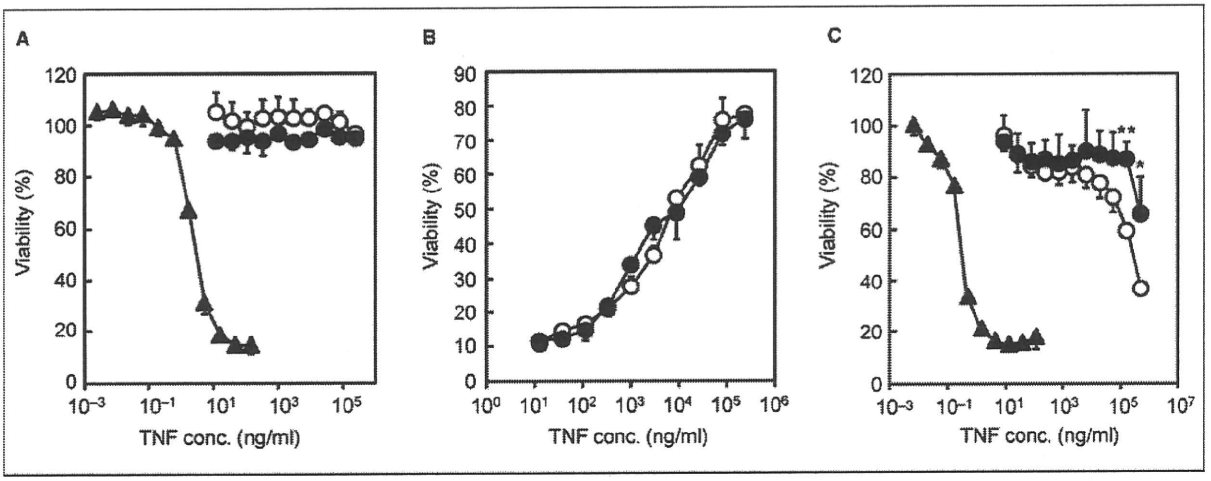

Fig.: Bioactivities and antagonistic activities of N7. (A) To determine the TNFR1-mediated bioactivities, several dilutions of wtTNF (closed triangle), mutTNF (open circle) and N7 (closed circle) were added to L-M cells and incubated for 4 h at 37 °C. (B) Indicated dilutions of mutTNF (open circle) and N7 (closed circle) and constant of wtTNF (5 ng/ml) were mixed and added to L-M cells and incubated for 4 h at 37 °C. TNFR1-mediated antagonistic activity was assessed as described in the Experimental section. (C) To determine the TNFR2-mediated bioactivities, diluted wtTNF (closed triangle), mutTNF (open circle) and N7 (closed circle) were added to hTNFR2/mFas-preadipocyte cells and incubated for 48 h at 37 °C. After incubation, cell viability was measured using the methylene blue assay. Data represent the mean ± S.D. and were analyzed by Student's t-test (*$p < 0,05$, **$p < 0,01$ vs mutTNF)

HEp-2 cells (Table). As anticipated, mutTNF was unable to activate TNFR1. Likewise clones N3 and N7 do not activate TNFR1 signaling, even when tested at high concentrations. The TNFR1-mediated antagonistic assay demonstrated that N7 showed the highest activity of all the TNFR1-selective antagonist candidates. The Figure show details of bioactivities and antagonistic activities of N7. The TNFR1-mediated agonistic activity using L-M cells showed that wtTNF displays TNFR1-mediated agonistic activity in a dose-dependent manner. In contrast, N7, in addition to mutTNF, barely displays any agonistic activity (Fig. A). Moreover, N7 had an almost identical antagonistic activity for TNFR1-mediated bioactivity to that of mutTNF (Fig. B). Next, TNFR2-mediated activities of these TNFR1-selective antagonists were measured using hTNFR2/mFas-preadipocyte cells. The bioactivity of mutTNF and N7 *via* TNFR2 was much lower than that of wtTNF. Remarkably, TNFR2-mediated agonistic activity of N7 was lower than that of mutTNF, in agreement with the reduced affinity for TNFR2 (Fig. C).

In conclusion, we have succeeded in creating a TNFR1-selective antagonist with improved TNFR1-selectivity over that of mutTNF. This was achieved by constructing a library of mutTNF variants using a phage display technique. While TNFR1 is believed to be important for immunological responses (Rothe et al. 1993), TNFR2 is thought to be important for antiviral resistance and is effective for controlling mycobacterial infection by affecting membrane-bound TNF stimulation (Saunders et al. 2005; Olleros et al. 2002). Therefore, use of N7 might reduce the risk of side effects, such as infections, when applying TNF blockade as a therapy for autoimmune disease. We are currently evaluating the therapeutic effect of N7 using a mouse autoimmune disease model.

3. Experimental

3.1. Cell culture

HEp-2 cells (a human fibroblast cell line) were provided by Cell Resource Center for Biomedical Research (Tohoku University, Sendai) and were maintained in RPMI 1640 medium supplemented with 10% FBS and 1% antibiotics cocktail (penicillin 10,000 units/ml, streptomycin 10 mg/ml, and amphotericin B 25 μg/ml). L-M cells (a mouse fibroblast cell line) were provided by Mochida Pharmaceutical Co. Ltd. (Tokyo, Japan) and were maintained in minimum Eagle's medium supplemented with 1% FBS and 1% antibiotics cocktail. hTNFR2/mFas-preadipocyte cells were established previously in our laboratory (Abe et al. 2008) and were maintained in Dulbecco's modified Eagle's medium supplemented with Blasticidin S HCl, 10% FBS, 1 mM sodium pyruvate, 5×10^{-5} M 2-mercaptoethanol, and 1% antibiotic cocktail.

3.2. Construction of a novel gene library displaying mutTNF variants

The pCANTAB phagemid vector encoding mutTNF was used as template for PCR. The mutTNF was created in previous study and showed TNFR1-selective antagonistic activity (Shibata et al. 2008b). The six amino acid residues at the receptor binding site (amino acid residues; 29, 31, 32 and 145–147) of mutTNF were replaced with other amino acids using a 2-step PCR procedure as described previously (Mukai et al. 2009).

3.3. Selection of TNFR1-selective antagonist candidates from a mutTNF mutated phage library

Human TNFR1 Fc chimera (R&D systems, Minneapolis, MN) was immobilized onto a CM3 sensor chip as described previously. Briefly, the phage display library (1×10^{11} CFU/100 μl) was injected over the sensor chip at a flow rate of 3 μl/min. After binding, the sensor chip was washed using the rinse command until the association phase was reached. Elution was carried out using 4 μl of 10 mM glycine-HCl. The eluted phage pool was neutralized with 1 M Tris-HCl (pH 6.9) and then used to infect *E. coli* TG1 in order to amplify the phage. The panning steps were repeated twice. Subsequently, single clones were isolated and supernatant from each clone was collected and used to determine the cytotoxicity in the HEp-2 cytotoxic assay and the affinity for TNFR1 by ELISA, respectively (Shibata et al. 2008b). We screened clones having almost no cytotoxicity but significant affinity for TNFR1. The phagemids purified from single clones were sequenced using the Big Dye Terminator v3.1 kit (Applied Biosystems, Foster City, CA). Sequencing reactions were analyzed on an ABI PRISM 3100 (Applied Biosystems).

3.4. Surface plasmon resonance assay (BIAcore® assay)

The binding kinetics of the proteins were analyzed by the surface plasmon resonance technique by BIAcore® (GE Healthcare, Amersham, UK). Each TNF receptor was immobilized onto a CM5 sensor chip, which resulted in an increase of 3,000–3,500 resonance units. During the association phase, all clones serially diluted in running buffer (HBS-EP) were allowed to pass over TNFR1 and TNFR2 at a flow rate of 20 μl/min. Kinetic parameters for each candidate were calculated from the respective sensorgram using BIAevaluation 4.0 software.

3.5. Cytotoxicity assay

In order to measure TNFR1-mediated cytotoxicity, HEp-2 or L-M cells were cultured in 96-well plates in the presence of TNF mutants and serially diluted wtTNF (Peprotech, Rocky Hill, NJ) with 100 μg/ml cycloheximide for 18 h at 4×10^4 cells/well or for 48 h at 1×104 cells/well. Cytotoxicity was then assessed using the methylene blue assay as described previously (Mukai et al. 2009; Shibata et al. 2004). For the TNFR1-mediated antagonistic assay, cells were cultured in the presence of 5 ng/ml human wtTNF and a serial dilution of the mutTNF. For the TNFR2-mediated cytotoxic assay, hTNFR2/mFas-preadipocyte cells were cultured in 96-well plates in the presence of TNF mutants and serially diluted wtTNF (1×10^4 cells/well) (Abe et al. 2008). After incubation for 48 h, cell survival was determined using the methylene blue assay.

Acknowledgement: This study was supported in part by Grants-in-Aid for Scientific Research from the Ministry of Education, Culture, Sports, Science and Technology of Japan, and by Grants-in-Aid for Scientific Research from Japan Society for the Promotion of Science (JSPS). In addition, this study was also supported in part by Health Labour Sciences Research Grants from the Ministry of Health, Labor and Welfare of Japan, Health Sciences Research Grants for Research on Publicly Essential Drugs and Medical Devices from the Japan Health Sciences Foundation and by a Grant from the Minister of the Environment, as well as THE NAGAI FOUNDATION TOKYO.

References

Abe Y, Yoshikawa T, Kamada H, Shibata H, Nomura T, Minowa K, Kayamuro H, Katayama K, Miyoshi H, Mukai Y, Yoshioka Y, Nakagawa S, Tsunoda S, Tsutsumi Y (2008) Simple and highly sensitive assay system for TNFR2-mediated soluble- and transmembrane-TNF activity. J Immunol Methods 335: 71–78.

Aggarwal BB (2003) Signalling pathways of the TNF superfamily: a double-edged sword. Nat Rev Immunol 3: 745–756.

Brown SL, Greene MH, Gershon SK, Edwards ET, Braun MM (2002) Tumor necrosis factor antagonist therapy and lymphoma development: twenty-six cases reported to the Food and Drug Administration. Arthritis Rheum 46: 3151–3158.

Feldmann M (2002) Development of anti-TNF therapy for rheumatoid arthritis. Nat Rev Immunol 2: 364–371.

Goldbach-Mansky R, Lipsky PE (2003) New concepts in the treatment of rheumatoid arthritis. Annu Rev Med 54: 197–216.

Gomez-Reino JJ, Carmona L, Valverde VR, Mola EM, Montero MD (2003) Treatment of rheumatoid arthritis with tumor necrosis factor inhibitors may predispose to significant increase in tuberculosis risk: a multicenter active-surveillance report. Arthritis Rheum 48: 2122–2127.

Grell M, Becke FM, Wajant H, Mannel DN, Scheurich P (1998) TNF receptor type 2 mediates thymocyte proliferation independently of TNF receptor type 1. Eur J Immunol 28: 257–263.

Imai S, Mukai Y, Takeda T, Abe Y, Nagano K, Kamada H, Nakagawa S, Tsunoda S, Tsutsumi Y (2008) Effect of protein properties on display efficiency using the M13 phage display system. Pharmazie 63: 760–764.

Kim EY, Priatel JJ, Teh SJ, Teh HS (2006) TNF receptor type 2 (p75) functions as a costimulator for antigen-driven T cell responses *in vivo*. J Immunol 176: 1026–1035.

Kim EY, Teh HS (2001) TNF type 2 receptor (p75) lowers the threshold of T cell activation. J Immunol 167: 6812–6820.

Kollias G, Kontoyiannis D (2002) Role of TNF/TNFR in autoimmunity: specific TNF receptor blockade may be advantageous to anti-TNF treatments. Cytokine Growth Factor Rev 13: 315–321.

Lubel JS, Testro AG, Angus PW (2007) Hepatitis B virus reactivation following immunosuppressive therapy: guidelines for prevention and management. Intern Med J 37: 705–712.

Mori L, Iselin S, De Libero G, Lesslauer W (1996) Attenuation of collagen-induced arthritis in 55-kDa TNF receptor type 1 (TNFR1)-IgG1-treated and TNFR1-deficient mice. J Immunol 157: 3178–3182.

Mukai Y, Shibata H, Nakamura T, Yoshioka Y, Abe Y, Nomura T, Taniai M, Ohta T, Ikemizu S, Nakagawa S, Tsunoda S, Kamada H, Yamagata Y, Tsutsumi Y (2009) Structure-function relationship of tumor necrosis factor (TNF) and its receptor interaction based on 3D structural analysis of a fully active TNFR1-selective TNF mutant. J Mol Biol 385: 1221–1229.

Nagano K, Imai S, Mukai Y, Nakagawa S, Abe Y, Kamada H, Tsunoda S, Tsutsumi Y (2009) Rapid isolation of intrabody candidates by using an optimized non-immune phage antibody library. Pharmazie 64: 238–241.

Nomura T, Kawamura M, Shibata H, Abe Y, Ohkawa A, Mukai Y, Sugita T, Imai S, Nagano K, Okamoto T, Tsutsumi Y, Kamada H, Nakagawa S, Tsunoda S (2007) Creation of a novel cell penetrating peptide, using a random 18mer peptides library. Pharmazie 62: 569–573.

Olleros ML, Guler R, Corazza N, Vesin D, Eugster HP, Marchal G, Chavarot P, Mueller C, Garcia I (2002) Transmembrane TNF induces an efficient cell-mediated immunity and resistance to Mycobacterium bovis bacillus Calmette-Guerin infection in the absence of secreted TNF and lymphotoxin-alpha. J Immunol 168: 3394–3401.

Rothe J, Lesslauer W, Lotscher H, Lang Y, Koebel P, Kontgen F, Althage A, Zinkernagel R, Steinmetz M, Bluethmann H (1993) Mice lacking the tumour necrosis factor receptor 1 are resistant to TNF-mediated toxicity but highly susceptible to infection by Listeria monocytogenes. Nature 364: 798–802.

Saunders BM, Tran S, Ruuls S, Sedgwick JD, Briscoe H, Britton WJ (2005) Transmembrane TNF is sufficient to initiate cell migration and granuloma formation and provide acute, but not long-term, control of Mycobacterium tuberculosis infection. J Immunol 174: 4852–4859.

Shibata H, Yoshioka Y, Ikemizu S, Kobayashi K, Yamamoto Y, Mukai Y, Okamoto T, Taniai M, Kawamura M, Abe Y, Nakagawa S, Hayakawa T, Nagata S, Yamagata Y, Mayumi T, Kamada H, Tsutsumi Y (2004) Functionalization of tumor necrosis factor-alpha using phage display technique and PEGylation improves its antitumor therapeutic window. Clin Cancer Res 10: 8293–8300.

Shibata H, Yoshioka Y, Ohkawa A, Abe Y, Nomura T, Mukai Y, Nakagawa S, Taniai M, Ohta T, Mayumi T, Kamada H, Tsunoda S, Tsutsumi Y (2008a) The therapeutic effect of TNFR1-selective antagonistic mutant TNF-alpha in murine hepatitis models. Cytokine 44: 229–233.

Shibata H, Yoshioka Y, Ohkawa A, Minowa K, Mukai Y, Abe Y, Taniai M, Nomura T, Kayamuro H, Nabeshi H, Sugita T, Imai S, Nagano K, Yoshikawa T, Fujita T, Nakagawa S, Yamamoto A, Ohta T, Hayakawa T, Mayumi T, Vandenabeele P, Aggarwal BB, Nakamura T, Yamagata Y, Tsunoda S, Kamada H, Tsutsumi Y (2008b) Creation and X-ray structure analysis of the tumor necrosis factor receptor-1-selective mutant of a tumor necrosis factor-alpha antagonist. J Biol Chem 283: 998–1007.

Yamamoto Y, Tsutsumi Y, Yoshioka Y, Nishibata T, Kobayashi K, Okamoto T, Mukai Y, Shimizu T, Nakagawa S, Nagata S, Mayumi T (2003) Site-specific PEGylation of a lysine-deficient TNF-alpha with full bioactivity. Nat Biotechnol 21: 546–552.

Expert Opinion

Tight junction modulator and drug delivery

Koji Matsuhisa, Masuo Kondoh†, Azusa Takahashi & Kiyohito Yagi
Osaka University, Graduate School of Pharmaceutical Sciences, Department of Bio-Functional Molecular Chemistry, Osaka, Japan

Recent progress in pharmaceutical technology based on genomic and proteomic research has provided many drug candidates, including not only chemicals but peptides, antibodies and nucleic acids. These candidates do not show pharmaceutical activity without their absorption into systemic flow and movement from the systemic flow into the target tissue. Epithelial and endothelial cell sheets play a pivotal role in the barrier between internal and external body and tissues. Tight junctions (TJs) between adjacent epithelial cells limit the movement of molecules through the intercellular space in epithelial and endothelial cell sheets. Thus, a promising strategy for drug delivery is the modulation of TJ components to allow molecules to pass through the TJ-based cellular barriers. In this review, we discuss recent progress in the development of TJ modulators and the possibility of absorption enhancers and drug-delivery systems based on TJ components.

Keywords: absorption enhancer, claudin, drug delivery, occludin, paracellular route, tight junction

Expert Opin. Drug Deliv. (2009) 6(5):509-515

1. Introduction

Drug candidates, including chemicals, peptides, proteins, nucleic acids and their derivatives, can be efficiently identified by a combination of high-throughput technology and genome-based drug discovery. However, two steps are required for the clinical application of these drug candidates: movement of the molecules into the body and tissue through epithelial and endothelial cell sheets. These cell sheets regulate the movement of solutes between tissues within the body as well as between the outside and inside of the body.

Routes for passing of drug through the epithelial and endothelial cell sheets are classified into transcellular and paracellular routes (Figure 1). In the transcellular route, drugs are delivered by simple diffusion into the cell membranes and active transport via a receptor or transporter on the cell membrane [1,2]. Various transporters involved in the influx and efflux of peptides, organic anions and cations have been identified, and transcellular delivery systems using the transporters have been widely investigated [2-6]. Transporter-mediated drug delivery is tissue-specific and has low toxicity; however, the drugs must be modified for interaction with the transporter without loss of pharmaceutical activity. Thus, the transcellular route is not suitable for high-throughput production of drug candidates. The other route for drug delivery is the paracellular route. Tight junctions (TJs) seal the paracellular route and prevent the free movement of molecules in the paracellular space; therefore, a strategy for the paracellular delivery of drugs is the opening of TJs [7,8]. Compared with the transcellular route, the paracellular route has the advantages that drug modification is not needed and that one method can be applied for various drugs. Drug delivery systems through the paracellular route have been investigated as absorption enhancers since the 1980s. However, only sodium caprate is currently used as an absorption enhancer in pharmaceutical therapy.

informa
healthcare

10.1517/17425240902902315 © 2009 Informa UK Ltd ISSN 1742-5247

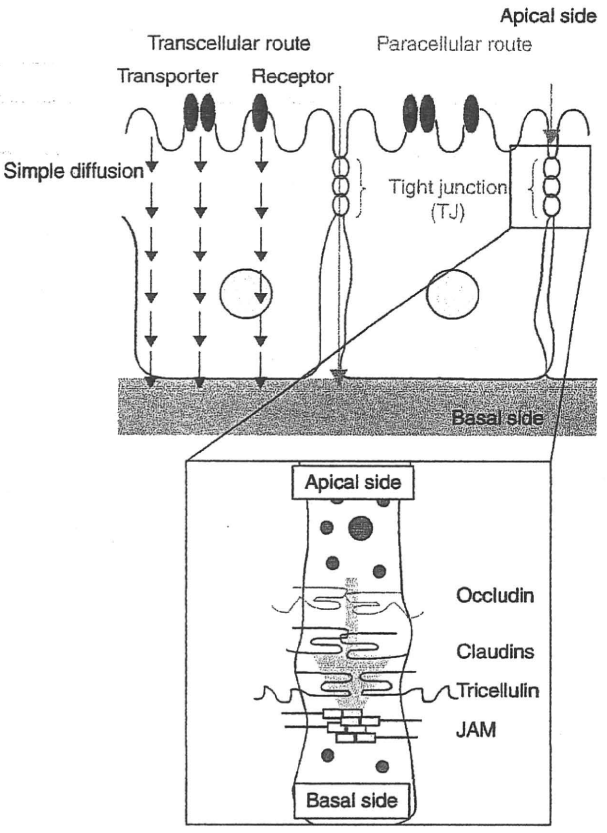

Figure 1. Schematic illustration of transport routes in epithelia.

It had been unclear how TJs regulated movement of solutes and what TJs were. In 1993, Furuse and colleagues determined that occludin, a protein with four transmembrane domains, is a component of TJs and that TJs consist of protein [9]. In 1998, Furuse and co-workers also identified another TJ protein, claudin-1 and -2 [10]. Claudins, a multigene family of at least 24 members, are key molecules of the TJ barrier [11]. Schematic biochemical machinery of TJs is shown in Figure 1, and modulation of the TJ components to allow drugs to pass through the paracellular route has been investigated as a novel strategy for drug delivery since the first report of TJ component-based drug delivery using an occludin peptide corresponding to part of the extracellular loop [12].

In this review, we examine recent topics in TJ-based drug delivery systems that use both approaches – TJ component/TJ modulator and TJ barrier – and discuss the future direction of such systems.

2. TJ components and TJ modulators

In the first section, we reviewed recent progress in TJ modulators over the past 2 years with respect to TJ components and modulators of TJ barrier.

2.1 Claudin

Claudin is a four-transmembrane TJ protein with a molecular mass of around 23 kDa, and comprises a family of at least 24 members [10]. Expression of each claudin member varies among cell types and tissues [13,14]. Claudins are thought to polymerize and form TJ strands in a homomeric and heteromeric manner, and the combination and mixing ratios of different claudin species determine the barrier properties of TJs, depending on the tissues [11]. For instance, deletion of claudin-1 causes dysfunction of the epidermal barrier [15], and deletion of claudin-5 causes dysfunction of the blood–brain barrier [16]. These findings indicate that a specific claudin modulator would be useful for tissue-specific drug delivery through the paracellular route. The C-terminal receptor binding region of *Clostridium perfringens* enterotoxin (C-CPE) is the only known modulator of claudin-4 [17]. Cells treated with C-CPE have decreased intracellular levels of claudin-4 as well as disrupted TJ barriers in epithelial cell sheets [17]. We previously found that the jejunal absorption-enhancing effect of C-CPE was 400-fold more potent than that of sodium caprate, the only clinically used absorption enhancer [18]. The development of other claudin modulators by using C-CPE as a prototype is a promising strategy. Deletion assays and site-directed mutagenesis assays indicate that the C-terminal 16 amino acids of C-CPE are involved in its modulation of claudin-4 and that Tyr residues at positions 306, 310 and 312 are critical for C-CPE activities [19,20]. Van Itallie and colleagues revealed that the structure of C-CPE is a nine-strand β sandwich and that the C-terminal 16–amino acid fragment is located in the loop region between the β8 and β9 strands, indicating that the claudin-4 binding site is on a large surface loop between strands β8 and β9 or on a domain containing these strands [21]. These findings indicate that peptides containing the loop structure formed by the β8 and β9 strands are likely to be novel claudin modulators. Considering the antigenicity of the claudin-4 modulator, smaller peptides are useful. Recently, the 12-mer peptide binders of claudin-4 were successfully identified using a random 12-mer peptide phage-display library [22]. The common claudin-binding motif <XX(Y/W)$(X)_{3\ or\ 4}$Y(Y/X)(L/I)XX> was also detected. The 12-mer peptide was bound to claudin with nanomolar affinity, but it did not modulate the claudin barrier. A 27-mer amino acid peptide corresponding to the extracellular loop region of claudin-1 modulated epithelial barrier through its interaction with claudin-3 [23]. Distinct species of claudins can interact within and between tight junctions [24]. Thus, a short peptide corresponding to the extracellular loop region of the heterotypically interacting claudin is also a candidate of claudin modulator.

2.2 Occludin

Occludin, a 65-kDa protein containing four transmembrane domains, was the first TJ-associated integral protein to be identified [9]. The initial strategy for TJ component-based